ORIGINAL ARTICLE

Endocannabinoid CB1 receptor-mediated rises in Ca^{2+} and depolarization-induced suppression of inhibition within the laterodorsal tegmental nucleus

Neeraj Soni · Kristi A. Kohlmeier

Abstract Cannabinoid type 1 receptors (CB1Rs) are functionally active within the laterodorsal tegmental nucleus (LDT), which is critically involved in control of rapid eye movement sleep, cortical arousal, and motivated states. To further characterize the cellular consequences of activation of CB1Rs in this nucleus, we examined whether CB1R activation led to rises in intracellular Ca^{2+} ($[Ca^{2+}]_i$) and whether processes shown in other regions to involve endocannabinoid (eCB) transmission were present in the LDT. Using a combination of Ca^{2+} imaging in multiple cells loaded with Ca^{2+} imaging dye via 'bulk-loading' or in single cells loaded with dye via a patch-clamp electrode, we found that WIN 55212-2 (WIN-2), a potent CB1R agonist, induced increases in $[Ca^{2+}]_i$ which were sensitive to AM251, a CB1R antagonist. A proportion of rises persisted in TTX and/or low-extracellular Ca^{2+} conditions. Attenuation of these increases by a reversible inhibitor of sarcoplasmic reticulum Ca^{2+}-ATPases, suggests these rises occurred following release of Ca^{2+} from intracellular stores. Under voltage clamp conditions, brief, direct depolarization of LDT neurons resulted in a decrease in the frequency and amplitude of AM251-sensitive, inhibitory postsynaptic currents (IPSCs), which was an action sensitive to presence of a Ca^{2+} chelator. Finally, actions of DHPG, a mGlu1R agonist, on IPSC activity were examined and found to result in an AM251- and BAPTA-sensitive inhibition of both the frequency and amplitude of sIPSCs. Taken together, our data further characterize CB1R and eCB actions in the LDT and indicate that eCB transmission could play a role in the processes governed by this nucleus.

Keywords LDT · Marijuana · Synaptic transmission · Ca^{2+} imaging · DSI · mGluR

Introduction

Marijuana or cannabis (*Cannabis sativa*) is the most commonly utilized illicit drug around the world. Psychoactive effects leading to its recreational and compulsive use are mediated by one of its principle constituents, Delta-9-tetrahydrocannabinol (THC), which activates the CB1R (Gaoni and Mechoulam 1964). Endogenously the CB1R is stimulated by production of natural endocannibinoids (eCBs) such as anandamide (Devane et al. 1992) and Sn-2-arachidonoyl-glycerol (2-AG) (Mechoulam et al. 1995; Sugiura et al. 1995, 1999). Synthesis of eCBs occurs 'on demand' with some evidence that eCBs can be presynthesized and stored (Alger and Kim 2011; Edwards et al. 2006; Min et al. 2010). Upon their release, eCBs activate CB1Rs to effect a variety of actions, including activation and suppression of membrane ion channels leading to increases or decreases in cellular excitability. Synthesis of eCBs can occur following depolarization of the postsynaptic cell and once produced, the eCBs act as a retrograde signal at CB1Rs located on presynaptic terminals. In this fashion, postsynaptic cells via their production of eCBs can inhibit the release of excitatory or inhibitory neurotransmitters from terminals. This eCB-mediated phenomenon is called depolarization-induced suppression of excitation (DSE) or depolarization-induced suppression of inhibition (DSI) (Diana et al. 2002; Kreitzer and Regehr 2001; Maejima et al. 2001; Wilson et al. 2001; Wilson and Nicoll

N. Soni · K. A. Kohlmeier (✉)
Department of Drug Design and Pharmacology, Faculty of Health and Medical Sciences, University of Copenhagen, Universitetsparken 2, 2100 Copenhagen, Denmark
e-mail: kak1@sund.ku.dk

2001) depending on whether the affected afferent inputs are glutamatergic or GABAergic, respectively.

The wide distribution of CB1Rs throughout the brain indicates that eCB transmission is involved in a host of neurobiological processes. CB1Rs are highly expressed in the hippocampus, cerebellum, striatum, basal ganglia (Berrendero et al. 1998; Mailleux and Vanderhaeghen 1992; Matsuda et al. 1993; Tsou et al. 1998), ventral tegmental area (VTA) (Melis et al. 2004; Perra et al. 2005) and the nucleus accumbens (NAc) (Robbe et al. 2001, 2002, 2003, 2006), among other neural regions. Their location within these areas likely underlies their demonstrated participation in memory processes, directed movement and motivated states (Fergusson and Horwood 2000; Iversen 2003; Serrano and Parsons 2011). We have recently shown that CB1Rs are functionally present in a pontine neuronal group, the laterodorsal tegmentum (LDT) and endogenous activation of these receptors is present in the brain slice (Soni et al. 2014). The LDT nucleus is comprised of cholinergic, glutamatergic and GABAergic neurons (Wang and Morales 2009). Arguably the most widely studied, the cholinergic neurons of the LDT have been demonstrated to play a key role in regulation of states showing an aroused, gamma-rich EEG, such as alert wakefulness and rapid eye movement sleep (REM) (el Mansari et al. 1989; Jones and Yang 1985; Kayama et al. 1992; Satoh and Fibiger 1986). A growing body of evidence suggests that neurons of the LDT are also critically involved in drug addiction behaviors (Forster and Blaha 2000; Lammel et al. 2012; Nelson et al. 2007). In support of the conclusion that eCB neural transmission is likely involved in processes controlled by the LDT, the psychobiological actions of marijuana and its psychoactive constituent, THC, include alterations in the sleep cycle, reductions in arousal and decreases in one component of sleep, REM sleep (Feinberg et al. 1975, 1976; Nicholson et al. 2004; Pivik et al. 1972), which are all phenomenon known to be controlled in part by the LDT. Effects of activation of CB1Rs within the LDT could also be expected to play a role in the reward experienced by use of marijuana. The LDT sends cholinergic projections to the VTA and the NAc (Dautan et al. 2014), midbrain regions critical in motivated behavior, with preferential innervation of the mesoaccumbal dopamine (DA)-containing neurons of the VTA (Omelchenko and Sesack 2005, 2006) and it is LDT input to the VTA which gates the high-frequency firing of DA-VTA cells (Lodge and Grace 2006) necessary for high DA efflux in the NAc associated with reward evaluation of motivating stimuli. Accordingly, activity of the eCB system within the LDT would be expected to alter the output of these cells to target regions within the VTA, and could by this action, influence reward processing.

We have shown that *CB1R* mRNA is present within the LDT, activation of CB1Rs in this nucleus results in reductions in the frequency of IPSPs directed to cholinergic LDT cells and CB1R stimulation induces a small, post-synaptic hyperpolarizing membrane current (Soni et al. 2014). In addition, we presented data suggestive of an ongoing CB1R-mediated inhibition of IPSC activity within mouse brain slices. Taken together, these data not only confirm the presence of CB1Rs in the LDT as suggested by detection of CB1R mRNA in this nucleus (Allen Mouse Brain Atlas 2012), but also indicate that these receptors are functional, and could, therefore, play a role in processes controlled by the LDT. However, further characterization of the cellular actions of CB1R stimulation on LDT neurons and a better understanding of eCB transmission within this nucleus is necessary to understand how eCB transmission is involved in processes controlled by the LDT. Accordingly, as activation of CB1Rs has been shown to modulate $[Ca^{2+}]_i$ in other cell types and levels of $[Ca^{2+}]_i$ are importantly involved in gene transmission and neuronal plasticity and in endogenous-generation of eCBs, we determined whether relative levels of Ca^{2+} of LDT neurons were altered by CB1R agonists using bulk-load Ca^{2+} imaging and single-cell imaging. Further, as from our earlier work we had evidence that eCBs were being produced and released in the slice (Soni et al. 2014), in this study, we determined using patch-clamp recordings from LDT neurons whether depolarization of these cells induced eCB-mediated alterations in synaptic input suggestive of DSI or DSE and the role played by Ca^{2+} in this phenomenon. Finally, as LDT neurons contain mGluRs and receive a substantial glutamatergic input (Kohlmeier et al. 2012), we determined whether activation of these receptors that have been shown in other cells types to elicit eCB production, resulted in eCB-mediated activity sufficient to induce alterations in synaptic currents. When taken together, our findings provide further knowledge of the cellular actions of eCB transmission in the LDT, which could include activation of Ca^{2+}-dependent processes and they suggest that the eCB system could play a role in modulating the synaptic activity of LDT neurons and by these actions, shape the processes governed by this nucleus.

Materials and methods

Animal use

Animal use studies were permitted by the Animal Welfare Committee, appointed by the Danish Ministry of Justice and animal studies complied with the European Communities Council Directive of 24 November 1986 (86/609/EEC) and Danish laws regulating experiments on animals.

Brain slice preparation

Preparation of LDT brain slices from 8-to 15-day-old NMRI wild-type mice (Harlan Mice laboratories, Denmark), which was the age used for the bulk of the studies in this report, was conducted as in previous studies (Kohlmeier et al. 2006). Since the CB1R is present early in postnatal development, (Berrendero et al. 1999; Fernandez-Ruiz et al. 1999), the age chosen was selected for two reasons: (1) successful multiple cell bolus loading with the Ca^{2+} indicator dye utilized is difficult within the LDT in slices from older animals and, (2) the protocols utilized for the patch-clamp recordings required long recording times, which were difficult to obtain with cells from older animals. However, evidence of phenomenon presented in the age range of 8–15 days, which involved CB1R activation, was also found in preliminary studies in a small number of cells tested ($n = 4$) from older animals (16–25 days of age). Prior to extraction of the brain, NMRI mice were anesthetized with isoflurane (100 %). The brain was then removed, and 250 μm thick coronal slices containing the LDT nucleus were cut using a cryostat (Leica VT 1200S, Leica, Germany) after reductions in vertical deflections were made (Vibrocheck, Leica). Dissections and sectioning were performed in ice-cold (0–4 °C) artificial cerebrospinal fluid (ACSF). ACSF contained (in mM): 124 NaCl, 5 KCl, 1.2 Na_2HPO_4, 2.7 CaCl2, 1.2 MgSO4, 10 glucose and 2.6 NaHCO3 and was bubbled with 95 % O_2 + 5 % CO_2 which resulted in a pH of 7.4 (295–300 mOsm). Slices were incubated in ACSF at 37 °C for 15–20 min and thereafter maintained at room temperature for 1 h prior to placement within the recording chamber.

Drugs

WIN-2 was used for these studies, as it is a synthetic potent agonist for the CB1R. WIN-2 (10 μM, Sigma-Aldrich, St Louis, MO, USA) is an analog of the psychoactive constituent of marijuana, Delta-9-THC, and exhibits a high efficacy when compared to that of other cannabinoid agonists (Burkey et al. 1997; Compton et al. 1992) and has, therefore, been one of the most widely used agonists of the CB1R in electrophysiology studies. AM251 (10 μM, Tocris, Bristol, UK) which is a potent CB1R antagonist was utilized to inhibit actions mediated by the CB1R (Gatley et al. 1996, 1997). Nifedipine was used as an antagonist of the L-type Ca^{2+} channel (10 μM, Tocris, Bristol, UK). Aliquots of WIN-2, AM251 and nifedipine were produced by dissolving drugs in DMSO and stock aliquots were stored at −20 °C until use. At time of use, the aliquot was dissolved in regular ACSF, ensuring that the final concentration of DMSO was less than 0.5 % which we have shown in previous studies does

not have actions on neurons of the LDT. In some experiments, low Ca^{2+} ACSF was utilized which consisted of 2.7 mM Ca^{2+} buffered with 2.7 mM EGTA, which effectively eliminates synaptic processes and membrane flux reliant on extracellular Ca^{2+} (Kohlmeier et al. 2004). As has been widely reported, effects of WIN-2 are slow to develop and, therefore, this agonist was applied for 5–10 min. In some experiments, the CB1R antagonist AM251 was applied for 2–3 min prior to the application of WIN-2. Tetrodotoxin (500 nM, Alomone Labs, Denmark) was used to inhibit voltage-gated Na^+ channels. sIPSCs were recorded with a patch solution optimized to visual inhibitory events and in the presence of bath-applied AP-5 (50 μM, Tocris, Bristol, UK) and DNQX (15 μM, Tocris, Bristol, UK) to block glutamatergic EPSCs. Ca^{2+} imaging was conducted using either the cell permeant acetoxymethyl (AM) ester form of Fura 2-AM or for single-cell studies using patch-clamp recordings, the cell impermeant form, *bis*-Fura-2 (Molecular Probes/Invitrogen, Denmark). The reversible inhibitor of sarcoplasmic reticulum Ca^{2+}-ATPase, Cyclopiazonic acid (CPA) (20 μM, Tocris, Bristol, UK) was used to deplete $[Ca^{2+}]_i$ stores. (S)-3,5-Dihydroxyphenylglycine (DHPG, 50 μM, Tocris, Bristol, UK) was used as a selective group I mGluR agonist. Chelation of $[Ca^{2+}]_i$ was conducted using 1,2-Bis (2-aminophenoxy) ethane-N,N,N',N'-tetraacetic acid tetrapotassium salt (BAPTA, 20 mM, Sigma, USA), which was added to the recording pipette solution.

Ca^{2+} imaging

Multiple-cell Ca^{2+} imaging

Effects of CB1R stimulation on $[Ca^{2+}]_i$ were monitored within the LDT nucleus using bulk-load Ca^{2+} imaging and single-cell Ca^{2+} imaging. For bulk-load imaging, LDT cells were loaded with the AM ester of the ratiometric Ca^{2+} indicator dye, Fura-2 by incubating slices in ACSF containing Fura 2-AM (15 μM, Molecular Probes, Invitrogen, USA) prepared from 3.3 mM stock of Fura 2-AM in DMSO. Slices were incubated for 10 min (plus 1 min for every day of the mouse postnatal age) at 36 °C in a small volume (5 ml) of solution in a test tube, which was covered with silver foil to reduce light exposure, equilibrated with carbogen (95 % O_2 + 5 % CO_2). After the dye incubation, slices were transferred to the recording chamber and were rinsed with ACSF for 10–15 min to ensure Fura 2-AM deesterification and room temperature equilibration. Localization of the LDT was made in bright-field illumination using the 4X objective of an upright microscope (Olympus BX51WI, Germany, Olympus Europe). Individual cells were then imaged using a 40× water immersion lens.
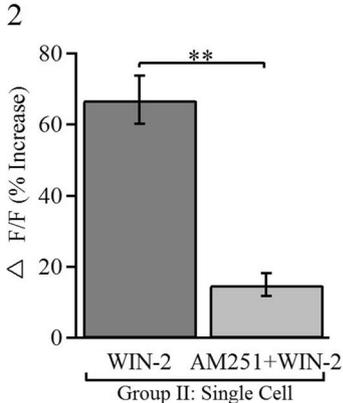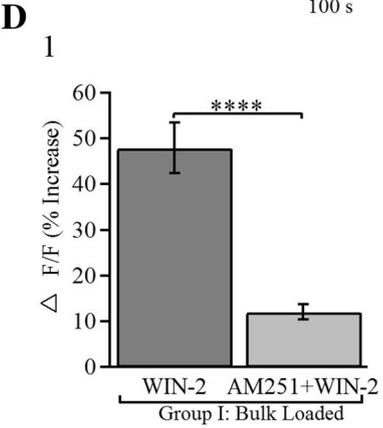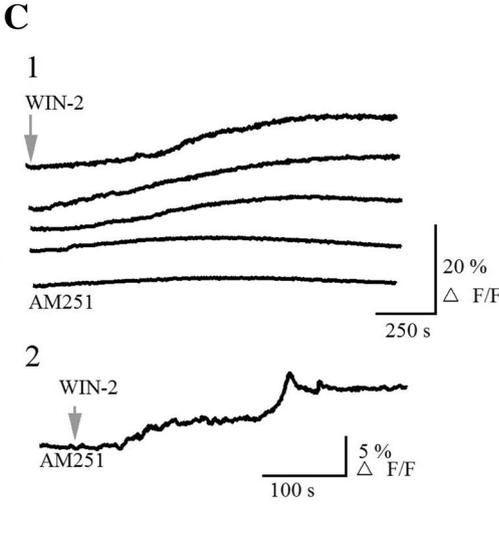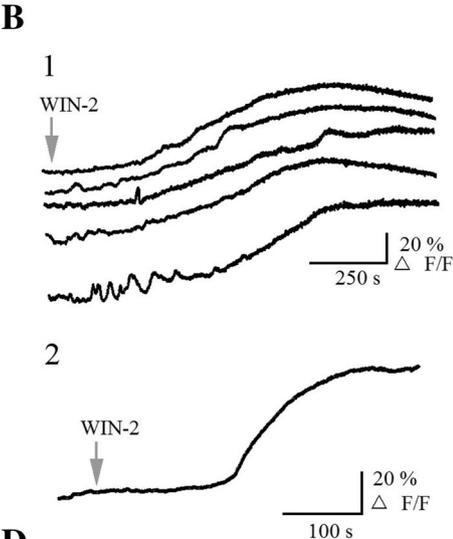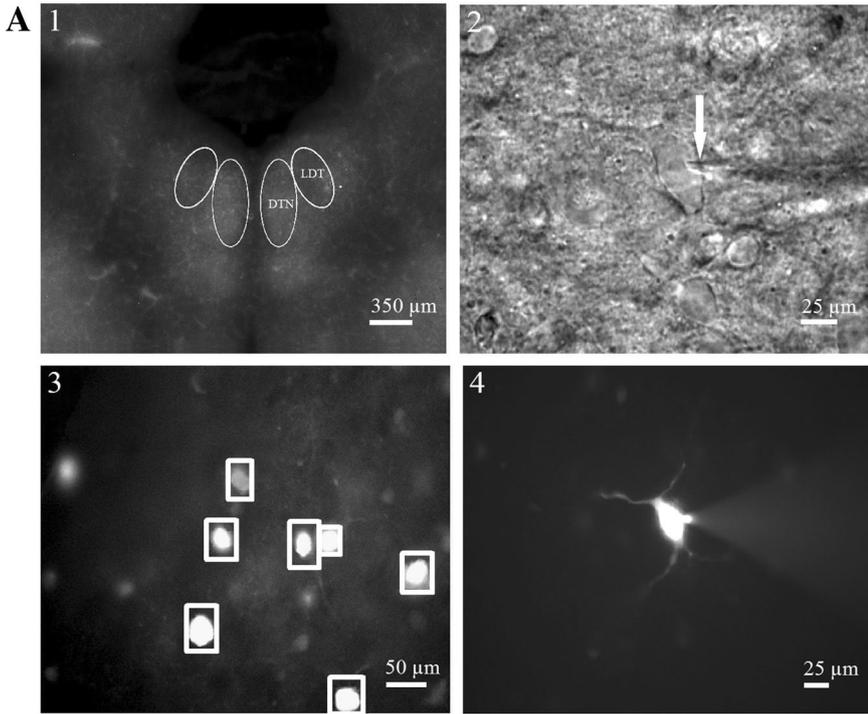
◄**Fig. 1** WIN-2 elicited rises in $[Ca^{2+}]_i$ within neurons of the laterodorsal tegmental nucleus (LDT). **a1** A representative image of a coronal mouse brain slice taken with low gain bright-field optics to show the LDT, from which changes in fluorescence of the Ca^{2+} indicator dye, Fura 2, were monitored using either bulk-load imaging, or single-cell imaging. The dorsal tegmental nucleus (DTN), which presents with a clearly visible perimeter just medial to the LDT and above the fourth ventricle is apparent and served as a reference point. **a2** Higher gain image of the LDT taken under bright-field optics in which a single neuron from the LDT was patch clamped with a pipette filled with *bis*-Fura-2 (*white-arrow*) which passively diffused into the cell during the recording. **a4** The same neuron as in **a2** viewed under 380 nm fluorescence in which changes in $\Delta F/F$ of *bis*-Fura-2 were monitored and used as an indirect measure of a change in $[Ca^{2+}]_i$. **a3** Neurons of the LDT nucleus in a Fura 2-AM bulk-loaded slice under fluorescent light (F380), where approximately five to six dye-filled cells can remain in focus. *Boxes* drawn around individual cells in **a3** indicate regions of interest (ROIs) drawn around the cells from which $\Delta F/F$ were measured. **b1** Representative samples of changes in fluorescence induced by WIN-2 application in Fura 2-AM bulk-loaded cells of the LDT shown in panel **a3** and **b2** the change in $\Delta F/F$ elicited upon WIN-2 application in a single LDT neuron (the same cell shown in panel **a4**) under whole-cell voltage clamp conditions at (-60 mV). **c1** Changes in $\Delta F/F$ induced by WIN-2 were significantly reduced from those obtained in control conditions when cells were pre-incubated with the CB1R antagonist, AM251 as shown in these representative traces from a population of bulk-loaded LDT cells. **c2** Single-cell recordings also indicated that rises in $\Delta F/F$ induced by WIN-2 were inhibited by presence of AM251. Note scale difference in **c** from that in **b**. **d** Histograms presenting the amplitude of the WIN-2-mediated change in $\Delta F/F$ from a group of bulk-loaded cells in control conditions compared with a different group of neurons pre-incubated with AM251 **d1**, as well as data from a population of patch-clamp, single-cell LDT neuron recordings (**d2**). Across the population of cells studied in both bulk (**d1**) and single-cell (**d2**) recording conditions, pre-incubation of the slice with the CB1R antagonist suppressed the rise in the $\Delta F/F$ ratio induced by WIN-2. *Error bars* indicate SEM and ***indicates $P < 0.01$ and ****indicates $P < 0.0001$

A CCD camera system (12 bit PCO Sensicam, Till photonics, Germany) attached to the microscope was used to monitor fluorescence of the dye. Regions of interest (ROIs, Fig. 1a3) were selected to encompass dye-filled cells within the LDT with appreciable processes. Collection of fluorescence within these ROIs was conducted, and the area within the ROI was binned at 2×2 with an exposure time of ~ 10–50 ms, selected to utilize less than 10 % of the full dynamic range, with an interval between image capture of 0.25–0.5 s. The excitation wavelength was automatically switched between 340 and 380 nm light using an ultrafast switch (Polychrome V, Till photonics, Germany) and the ratios of these signals were calculated following subtraction of background fluorescence as determined from a region of the field devoid of cells. Fura 2-AM bound to free $[Ca^{2+}]_i$ emits more when excited by 340 nm than it does when excited by 380 nm, so a rise in the ratio F_{340}/F_{380} corresponds to a rise in free $[Ca^{2+}]_i$. Changes in Ca^{2+} are inferred indirectly by measures of the relative increase in $\Delta F/F$ calculated as the maximum

$\Delta F/F$ during drug application. Baseline fluorescence, which was determined to be fluorescence at rest before application of any drugs, was subtracted for final determination of the drug-induced change in fluorescence (ΔF). Only those recordings of cells in which the F_{340}/F_{380} ratio remained stable, and did not change within a period exceeding 2 min before WIN-2 were included in the analysis, and cells were discounted in analysis if non-stable fluctuations in $\Delta F/F$ occurred after drug was applied and precluded confident determination of a drug-mediated change in $\Delta F/F$. Cells failing to respond with more than a 4 % change in $\Delta F/F$ were classified as non responders. The software LA acquisition (Till Vision Software, Germany) was used to control the CCD camera and collect the data. Offline analyses were conducted using an offline analysis tool in LA acquisition (Arrives Browser; Till Photonics, Version 4.2, Germany), and custom written macros in Igor Pro 6.2 (Wavemetrics, USA). All results are presented as mean $\pm$ SEM.

Single-cell Ca^{2+} imaging

For single-cell Ca^{2+} imaging, neurons were loaded with the Ca^{2+} imaging dye via the patch-clamp pipette. Whole-cell voltage clamp recordings of visualized LDT neurons were obtained as previously described (Ishibashi et al. 2009). Pipettes were filled with a recording solution containing (in mM) 144 K-gluconate, 3 MgCl2,10 HEPES, 0.3 NaGTP, and 4 Na2ATP (300–305 mOsm) including Alexa-594 (25 μM, Molecular Probes, Invitrogen, USA) and EGTA was replaced with *bis*-fura-2 (50 mM, Molecular Probes, Invitrogen, USA), which was dissolved in the patch pipette solution and allowed to passively diffuse into the cell. After establishing a whole-cell patch configuration, the cell was held at -60 mV in voltage clamp for a minimum of 10 min before imaging began. This allowed diffusion of dye and allowed dye to reach equilibrium in the neuronal processes. The response in fluorescence to changes in $[Ca^{2+}]_i$ produced by *bis*-fura-2 is nearly equivalent to changes induced in fluorescence of Fura-2AM, the dye used in bulk-load imaging (Naraghi 1997; Takahashi et al. 1999). Electrophysiological data were recorded with an amplifier Axopatch 200B (Molecular Devices: Axon Instruments, USA) (filtered at 2 kHz and digitized at 20 kHz). Liquid junction potentials were measured between the K-gluconate internal patch solutions and the extracellular ACSF solution, according to the method of Neher (Neher 1992) and measurements were not corrected for this potential (-9.1 mV). After establishing the whole-cell patch configuration in voltage clamp mode, series resistance and capacitance compensation (70–80 %) were performed by reducing the amplitude of the transient resulting from a brief voltage step. After at least 10 min to

allow diffusion of the dye within the cell, the recordings were switched to current clamp mode so that the resting membrane potential could be measured and only cells in which a stable potential of -55 to -60 mV without necessity of holding currents to maintain this voltage were included in this study. Further, it was confirmed in current clamp mode that patched cells were neurons by injection of a brief, depolarizing pulse (50 pA, 300 ms) sufficient to elicit action potentials. Image acquisition was controlled by a TTL pulse from the amplifier digitizer (Axon CNS 1440A, Molecular Devices, USA). Fluorescent measurements were started 10 s before any electrical protocols were applied to the cell. For single-cell imaging, exposure rates of 50–100 ms were utilized with intervals of 50–100 ms between frame pair capture. In studies of the effects of CB1R activation on L-type Ca^{2+} channels using measures of fluorescence, a long-duration depolarizing step from -60 to -30 mV for 5 s was utilized which we have previously shown elicits a Ca^{2+} rise with a large component of contribution from the L-type Ca^{2+} channel (Kohlmeier et al. 2006).

Electrophysiology

Synaptic currents from LDT neurons were recorded with an Axopatch 200B amplifier (Molecular Devices: Axon Instruments, USA) operated in whole-cell voltage clamp mode, and all recorded membrane currents were filtered at 2 kHz (low-pass Bessel filter) at the amplifier output and digitized at 20 kHz, analyzed using Clampex (Version 10.3, Molecular Devices, USA). For recordings designed to monitor inhibitory activity, patch pipettes (3–5 MΩ, Sutter P-97, Sutter Instruments, USA) were used which contained (in mM) 144 KCl, 0.2 EGTA, 3 MgCl2, 10 HEPES, 0.3 NaGTP, and 4 Na$_2$ATP, with an osmolarity range between 300 and 305 mOsM. This solution was used to reduce the drive for chloride into the cell, thereby giving rise to inwardly deflecting inhibitory events. In a separate group of recordings, to examine the Ca^{2+} dependence of DSI within LDT neurons, the Ca^{2+} buffer BAPTA (20 mM) was included in the high Cl^- internal patch solution. To elicit DSI, a depolarization step was initiated 5 min after achieving the whole-cell configuration in which the cell was stepped from the holding potential of -60 to 0 mV for a total duration of 5–10 s (1 stimulus). Liquid junction potentials were measured between the high Cl^- internal patch solution and the extracellular ACSF solution according to the method of Neher (Neher 1992) and values reported were not corrected for these junction potentials (2.8 mV). Recordings were not included in the analysis if holding currents exceeded -50 pA and if series resistance increased by more than 30 MΩ, which was monitored continuously.

Immunohistochemistry for bNOS positive cells

The LDT contains a mixed population of GABAergic, glutamatergic, and cholinergic neurons (Wang and Morales 2009). Although not an absolute predictor of phenotype, the cholinergic and glutamatergic neurons tend on average to be larger (>15 μm) in this nucleus (Boucetta et al. 2014; Boucetta and Jones 2009). Accordingly, to facilitate obtaining recordings in this study from these neuronal types, we targeted cells with soma sizes exceeding 15 μm. To identify the phenotype of the recorded cell after whole-cell patch recordings as cholinergic or not, we included Alexa-594 in patch pipettes, which could be located post hoc. Tissue was counter reacted with an antibody for brain nitric oxide synthase (bNOS) which is co-localized with choline acetyltransferase (ChAT) in neurons within the LDT nucleus (Hope et al. 1991; Vincent et al. 1983). Accordingly, bNOS is considered a reliable marker for cholinergic neurons in this nucleus and based on experience, is more consistently detected in brain slices in which hours of electrophysiology have been performed than markers designed to identify acetylcholine-synthesizing enzymes (Christensen et al. 2014). After recordings, slices were fixed in 4 % paraformaldehyde and then stored in phosphate buffer saline (PBS) for further processing. Slices were resectioned using a Leica cryostat CM 3050S (Leica, Germany) to 40 μm for immunohistological procedures. Slices were exposed to mouse monoclonal anti-bNOS antibody (rabbit polyclonal, Cat no: N7280, Sigma-Aldrich, Denmark) and subsequently, isothiocyanate (FITC)-labelled secondary antibody (Alexa Fluor 488, goat anti-rabbit IgG, Cat no: A11008, Molecular Probes/Invitrogen, Denmark) directed against the primary. Mounted slices were examined for both bNOS and Alexa-594 positive cells visualized using green–red filter for 488 and 594 nm wavelengths to detect green and red-fluorescent labelled bNOS and Alexa-594, respectively. All filters were set on an epifluorescence microscope (Axioskop 2, Zeiss) fitted with a monochrome CCD digital camera (Axiocam MRM, Zeiss, Germany). Images were collected using Axiovision 4.6 (Zeiss) software. Those cells positive for both indicators were determined to be recorded cells that were cholinergic; whereas, absence of bNOS in the Alexa-594 + cell indicated that the recorded cell was non-cholinergic.

Data analysis

All Ca^{2+} imaging data were exported in Microsoft excel format and agonist/antagonist-induced changes in fluorescence were measured using custom macros in Igor Pro 6.2 (Wavemetrics, USA). Determination of the statistical significance of effects of WIN-2 under different experimental

conditions was conducted by use of the two-tailed unpaired Student's *t* test (GraphPad Prism Version 6.01, GraphPad Software, Inc., CA, USA), where 'n' reported corresponds to the number of cells affected/numbers of cells sampled. Reported averages source from affected cells. Significant differences between the frequency and amplitude of sIPSCs and mIPSCs measured before and after drug (180 s) application were detected using Kolmogorov–Smirnov statistics (K–S test; Minianalysis, Ver 6.0.7, Synaptosoft Inc., NJ, USA). To compare the effect on synaptic events in a group of cells, Student's *t* tests (two-tail, paired, with significance set at $P < 0.05$) were performed using Graphpad prism (Version 6.01, GraphPad Software, USA). These data are presented as mean ± standard error of mean (SEM). The percentage change reported (% Con-Treatment/Control) represents the increase/decrease of the relative mean ± SEM for the population of cells that exhibited significance using the K–S test (n = the number of cells which exhibited significance in the K–S test/number of the entire population of cells recorded). In some experimental conditions, where cells could not serve as their own controls, a significant difference in the numbers of responsive and non-responsive cells from control conditions were analyzed by a 2×2 contingency table using a non-parametric test (Fisher test, two sided, with significance set at $P < 0.05$) with Graphpad prism (Version 6.01, GraphPad Software, USA). *P* values are represented as follows: $*P \leq 0.05$; $**P \leq 0.01$; $***P \leq 0.001$; $****P \leq 0.0001$.

Results

The CB1 receptor agonist, WIN-2, induces a change in intracellular Ca^{2+} within LDT neurons

Stimulation of the CB1R has been shown to induce neuronal $[Ca^{2+}]_i$ in regions where it has been examined. To investigate whether a similar effect occurs in LDT neurons, our first studies were designed to rapidly assay in a large number of LDT cells whether WIN-2, a CB1R agonist, altered $[Ca^{2+}]_i$ levels. Fura 2-AM is useful to load cells non-invasively as it readily crosses cell membranes, and several cells within a slice can be loaded simultaneously. This dye exhibits alterations in fluorescence with changes in levels of $[Ca^{2+}]_i$ allowing it to be used as an indirect measure of Ca^{2+} kinetics and this dye has previously been used to show agonist-induced changes in $[Ca^{2+}]_i$ in LDT neurons (Kohlmeier et al. 2004). Accordingly, we used 'bulk-load' Ca^{2+} imaging to monitor WIN-2 induced changes in $[Ca^{2+}]_i$ in LDT cells. Within each slice, at least four to five cells filled with the dye in the LDT and changes in fluorescence in the dye within these cells to WIN-2 could be monitored (Fig. 1a1, 3). WIN-2 (10 μM) induced

rises in florescence with an average $\Delta F/F$ of 48.0 ± 5.6 % in 77 % of recorded cells (n = 61/79; Fig. 1b1, d1). In another series of experiments, patch-clamp recordings were conducted of single cells identified as neurons by the presence of action potentials and *bis*-fura-2 dye was introduced via the patch pipette allowing the monitoring of change in $[Ca^{2+}]_i$ in individual neurons (Fig. 1a2, 4). WIN-2 caused rises in $[Ca^{2+}]_i$ in 78 % of the patch-clamped neurons with an average $\Delta F/F$ of 67.0 ± 6.7 % (n = 7/9; Fig. 1b2, d2). These data indicate that CB1 receptor activation has actions on the levels of $[Ca^{2+}]_i$ in a majority of LDT neurons.

The CB1R antagonist, AM251 suppresses, the WIN-2-induced increase in intracellular Ca^{2+}

The WIN-2-induced rise in $[Ca^{2+}]_i$ could be due to non-specific actions of WIN-2 as CB1R receptor independent actions of WIN-2 have been noted (Oz 2006a, b). Therefore, to determine whether effects of WIN-2 were specific to activation of CB1Rs, responses to WIN-2 were examined following preincubation of the brain slice with the CB1R antagonist, AM251 (10 μM). In the presence of AM251, which did not itself affect $[Ca^{2+}]_i$ as no changes were noted in fluorescence upon its application (data not shown), the WIN-2-induced increase in $\Delta F/F$ was significantly smaller than that obtained with WIN-2 alone in Fura 2-AM-loaded slices. In the presence of AM251, the WIN-2-induced increase was 25 % of that obtained in control conditions ($\Delta F/F$: 12.0 ± 1.6 %; n = 36/36; Fig. 1c1, d1). Paralleling the findings using bulk-loading, single-cell Ca^{2+} imaging with patch-clamped neurons revealed that pretreatment of the slice with AM251 resulted in a significantly smaller WIN-2-elicited rise of $\Delta F/F$ with a reduction of 77.0 ± 5.3 % from that obtained in control conditions (AM251 + WIN-2: Average $\Delta F/F$ 15 ± 3.2 %; n = 6/6, Fig. 1c2, d2). Taken together, our data suggest that WIN-2 induces rises in $[Ca^{2+}]_i$ mediated by specific actions at CB1Rs.

A component of the WIN-2-induced increase in intracellular Ca^{2+} was TTX insensitive

In the next series of experiments, we wanted to investigate whether the elevation of $[Ca^{2+}]_i$ induced by the CB1R agonist was dependent on action potentials generated within the slice. Accordingly, we performed our next studies using TTX in the bath, which selectively blocks voltage-dependent Na^+ channels and eliminates action potential generation. Following a 5 min incubation of the slice with TTX, WIN-2 was applied and we found a significantly smaller rise in the $\Delta F/F$ elicited by the CB1R agonist when compared to rises elicited in control

conditions. In the presence of TTX, the WIN-2-mediated rise in $\Delta F/F$ was reduced to 42.0 ± 13.0 % of that obtained with WIN-2 alone (WIN-2 + TTX: $\Delta F/F$ 15.0 ± 1.2 %, $n = 62/70$; Student's t test; $P < 0.0001$; Fig. 2a). This suggests that a portion of the WIN-2-induced elevation in $[Ca^{2+}]_i$ requires the generation of action potentials and is likely mediated by a non-terminally located presynaptic component. However, in addition, our findings indicate that one component of the WIN-2-mediated rise in $\Delta F/F$ is not reliant on action potentials and therefore likely stems from activation of CB1Rs in close proximity to the recorded cells which could be located on terminals presynaptic to the recorded cells or could be located postsynaptically and on the recorded cell. While the action potential-dependent CB1R-induced Ca^{2+} remains of interest, elucidation of the mechanisms involved in these Ca^{2+} rises seemed beyond the scope of this manuscript, as we wished to focus on very local circuit events in the LDT and this Ca^{2+} could have originated from actions at CB1Rs located outside the LDT. Therefore, the non-action potential-dependent component, which suggested a terminal or postsynaptic source, was the component upon which we chose to focus the next series of imaging studies.

A component of the WIN-2-induced increase in intracellular Ca^{2+} was CPA sensitive

Ca^{2+} rises could be due to a CB1R-induced activation of membrane Ca^{2+} channels in the postsynaptic cell, although CB1R activation is mostly commonly associated with inhibition of these channels (Brown et al. 2004; Caulfield and Brown 1992; Mackie and Hille 1992; Mackie et al. 1995) or, alternatively, release of Ca^{2+} stored in the endoplasmic reticulum (ER) within the cytoplasm of cells (Lauckner et al. 2005, 2008). In addition, although one component of Ca^{2+} increases persisted in presence of TTX, Ca^{2+} rises in the imaged cells could result from processes induced by
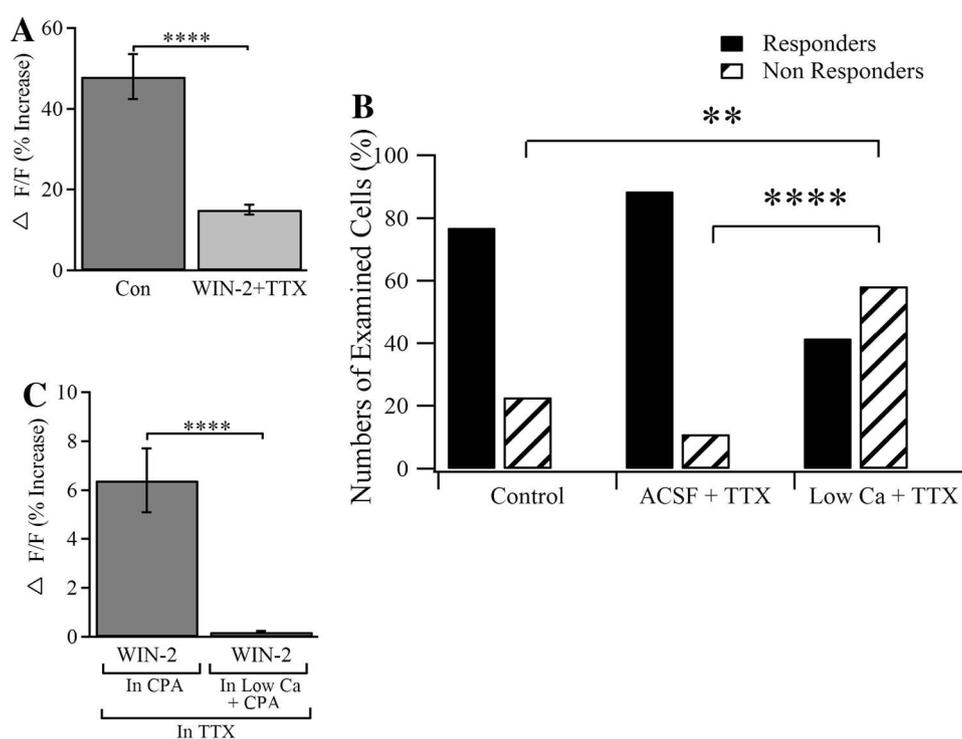
Fig. 2 WIN-2 induced changes in intracellular Ca^{2+} were contributed partially by a postsynaptic component. **a** Histogram from a group of neurons recorded in the LDT using bulk-load Ca^{2+} imaging indicating that while bath application of TTX suppressed a proportion of WIN-2-mediated changes in $\Delta F/F$ elicited in control conditions (*dark grey*), rises in Ca^{2+} were still apparent in presence of inhibition of action potential generation in the slice by inclusion of TTX (*light grey*). **b** A portion of responses persisted in conditions of synaptic blockade indicating they did not rely on synaptic transmission. The proportion of cells failing to respond to WIN-2 in low Ca^{2+} ACSF was significantly different than the proportion not responding to WIN-2 in control conditions (Control ACSF: 18/79 and ACSF + TTX: 8/70 failed to respond; Low Ca^{2+} + TTX: 14/24 failed to respond; $P = 0.002$ and $P = 0.0001$, Fisher Exact test, two tailed). **c** In a subset of cells in conditions of low Ca^{2+}/TTX and inclusion of CPA, which depletes $[Ca^{2+}]_i$, WIN-2 rises in $[Ca^{2+}]_i$ were abolished. Taken together, these data indicate that a portion of WIN-2-mediated Ca^{2+} is independent of both synaptic transmission and flux across the membrane and is mediated by release of Ca^{2+} from intracellular stores. *Error bars* indicate SEM, ** and ****indicate $P < 0.01$ and $P \leq 0.0001$, respectively

stimulation of proximally located presynaptic CB1Rs. Accordingly, we examined whether Ca^{2+} rises occurred in the presence of TTX and a low Ca^{2+} external solution, which produced a condition of synaptic blockade, and eliminated the flux of Ca^{2+} across the membrane. In low Ca^{2+}+TTX, 58.3 % of the recorded cells failed to respond to the agonist WIN-2 (14/24 cells), which was a significantly larger proportion of cells than the proportion which failed to respond to WIN-2 in control conditions (non responsive in normal ACSF 18/79 (22.7 %); $P = 0.002$, Fisher Exact test). Further, the proportion of non responding cells in low Ca^{2+}+TTX was significantly higher than the numbers of cells which failed to respond in TTX [non responsive in presence of TTX, 8/70 (11.4 %); $P = 0.0001$, Fisher Exact test] (Fig. 2b). However, in another group of cells, responses were present and the mean amplitude of the responses were not different from that obtained in control conditions ($\Delta F/F$ 55.0 ± 7.1 %; $n = 10/24$; $P > 0.05$), indicating that these rises were independent of flux of Ca^{2+} across cellular membranes.

Independence of Ca^{2+} flux across cellular membranes suggested that WIN-2-induced changes in $\Delta F/F$ could be due to release of Ca^{2+} from ER stores as this mechanism has been shown to occur in other cell types. Therefore, to test whether intracellular Ca^{2+} stores play a role in WIN-2-mediated rises, we examined the actions of CPA, which is an antagonist of sarcoendoplasmic reticulum Ca^{2+} (SERCA) pumps, on WIN-2-induced rises. Following pretreatment of the slices with CPA for 5 min, which we have shown is an effective time for emptying of the intracellular SERCA-pump mediated Ca^{2+} stores in cells of the LDT as evidenced by rises in $\Delta F/F$ (Kohlmeier et al. 2004) which return to a stable baseline, WIN-2-mediated increases in Ca^{2+} were found to be 77.0 ± 7.7 % lower in the majority of cells which was significant from changes in $\Delta F/F$ noted in control conditions (In presence of CPA + TTX: $\Delta F/F$ 6.4 ± 1.3 %; $n = 23/30$; $P < 0.0001$; Fig. 2c). We then examined WIN-2-mediated rises in intracellular Ca^{2+} in presence of low Ca^{2+} ACSF + TTX and CPA, and found that WIN-2-mediated responses were eliminated ($\Delta F/F$ 0.21 ± 0.04 %; $n = 62/75$, $P = 0.2038$; Fig. 2c). Our data indicate that WIN-2 leads to rises in Ca^{2+} that are due, in part, to release of Ca^{2+} from internal stores. Summarizing our Ca^{2+} imaging experiments, we determined that activation of CB1Rs within a local synaptic network in the LDT results in actions on Ca^{2+}, and these actions involve both flux across the membrane from a Ca^{2+} permeable source and release from intracellular stores, which are novel findings. However, with the bolus loading technique, it was difficult to extract further specific information about Ca^{2+} changes induced by CB1R activation, therefore, with the positive finding of alterations in

Ca^{2+} due to CB1R activation, we went further and conducted our next investigations using patch-clamp recordings to elucidate the involvement of Ca^{2+} in CB1R-mediated cellular actions.

WIN-2 induces an inhibition of the L-type Ca^{2+} current

Reductions of intracellular Ca^{2+} induced by CB1R activation in low Ca^{2+} solutions suggested the involvement of a Ca^{2+} permeable conductance. Activation of CB1Rs has been shown to result in inhibition of voltage-gated Ca^{2+} channels (VGCC) in many different neuronal regions and this inhibition likely plays a role in presynaptic inhibition stimulated via retrograde signaling (Freund et al. 2003; Howlett 2005; Kreitzer and Regehr 2001). Therefore, we wished to investigate effects of CB1R activation on a specific Ca^{2+} conductance known to be present in LDT cells: the L-type Ca^{2+} channel. Inhibition of the L-type VGCC following CB1R activation has been found to occur in retinal bipolar cells (Straiker et al. 1999; Straiker and Sullivan 2003) and neonatal rat solitary tract cells (Endoh 2006). The L-type Ca^{2+} channel in the LDT has been shown to be modulated by a variety of neuroactive compounds acting at G-protein coupled receptors, and has been shown to greatly influence the excitation of these cells (Kohlmeier and Leonard 2006) so it seemed feasible that CB1R activation could modulate function of this channel in the LDT. Accordingly we examined whether CB1R activation influenced functioning of the L-type Ca^{2+} channel using patch-clamp recordings of LDT neurons combined with simultaneous Ca^{2+} imaging. We utilized previously established protocols in which a long-lived depolarizing step of current was applied via the patch pipette to activate the L-type Ca^{2+} channel (Kohlmeier et al. 2008). Therefore, cells were depolarized from a holding potential of −60 to −30 mV for 5 s while Ca^{2+} imaging was being conducted. The resulting fluorescent transient has been shown to contain a significant contribution of Ca^{2+} from entry via L-type Ca^{2+} channels. WIN-2 was found to inhibit the Ca^{2+} conductance resulting from this step by approximately 71.0 ± 12.2 % of control ($\Delta F/F$ % Con: 54.1 ± 14.0; WIN2: 13 ± 4.9 %, $n = 4/4$; $P = 0.0357$; Fig. 3a, b). In a different group of cells, we tested the actions of nifedipine alone, the L-type Ca^{2+} channel antagonist and found that nifedipine reduced the transient to nearly the same extent ($\Delta F/F$ % Con: 54.1 ± 14.0; nifedipine: 14.0 ± 3.2 %, $n = 4/4$, $P = 0.0390$; Fig. 3c). We then tested the effect of WIN-2 and nifedipine on the fluorescent signal induced by the long-duration depolarizing step. We found that in the presence of the L-type Ca^{2+} channel antagonist, WIN-2 failed to significantly reduce the transient from the reduction seen in nifedipine alone
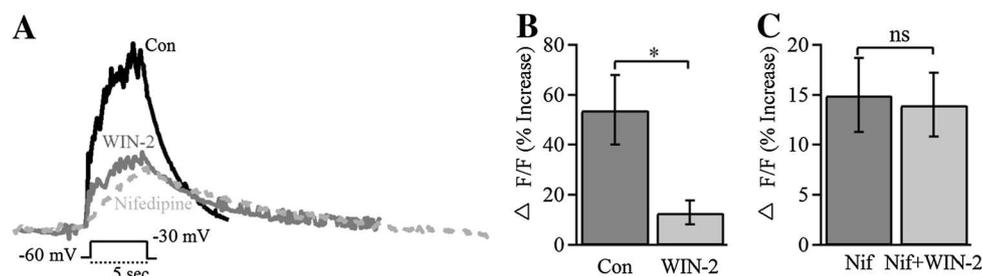
Fig. 3 WIN-2 suppresses the L-type Ca^{2+} conductance within the LDT. **a** Using voltage protocols shown to elicit a significant rise in $\Delta F/F$ mediated by L-type Ca^{2+} channels in LDT neurons, individual responses of $\Delta F/F$ are shown in control conditions (*black*), following exposure to WIN-2 (*dark grey*) and in presence of nifedipine (*broken line*), which reveal that WIN-2 induces a similar reduction in $\Delta F/F$ induced by this protocol as the L-type Ca^{2+} channel blocker. **b** Data from the population of patch-clamped cells in which the L-type Ca^{2+}

channel stimulation protocol was applied, indicating that WIN-2 significantly inhibited the rise in $\Delta F/F$ stimulated by the depolarizing step. **c** In a group of cells, WIN-2 failed to induce a significant decrease in $\Delta F/F$ when nifedipine was present, indicating occlusion of the WIN-2-mediated action by the L-type Ca^{2+} channel blocker. *Error bars* indicate SEM and * ndicates $P < 0.05$, whereas 'ns' designates lack of significance

control conditions in the same cells ($\Delta F/F$ % Nifedipine alone: 15.1 ± 3.7; WIN-2 + nifedipine: 14 ± 3.2 %, $n = 2/2$, $P = 0.8924$; Fig. 3c), suggesting occlusion of the action of WIN-2 by L-type Ca^{2+} channel blockade. Accordingly, our data indicate that WIN-2 has actions on L-type Ca^{2+} channels in LDT neurons and suggest that activation of CB1Rs would result in inhibition of Ca^{2+} entering these channels subsequent to their depolarization-triggered opening.

Depolarization-induced suppression of inhibition (DSI) occurs in the LDT and involves the CB1R

In a previous study, we found that activation of the CB1R resulted in a reduction in the frequency of inhibitory synaptic currents (sIPSCs) directed to LDT neurons (Soni et al. 2014). This effect was reminiscent of the CB1R-involved process known as DSI, which has been shown in other cell types to be induced by sustained depolarization of neurons, probably subsequent to endogenous production of eCBs from the postsynaptic cell acting at CB1Rs located on presynaptic input. We wished to test whether depolarization of LDT neurons could result in a similar phenomenon. Accordingly, in the presence of glutamate receptor blockers, and using a high Cl^- patch solution (E_{Cl} close to ~ 0 mV) in which the reversal potential for chloride had been altered such that downward going deflections in the recordings reflected inhibitory events, we measured the frequency and amplitude of sIPSCs before and following application of a single, long-lived depolarizing step (10 s, to a holding of 0 mV). We found that this protocol induced a significant change in both the frequency and amplitude of sIPSCs measured within 120 s after the stimulus in 80 % of the cells tested. Direct depolarization of LDT neurons resulted in a reduction in the mean frequency of sIPSCs to

33.0 ± 9.4 % of control (pre stimulus: 0.89 ± 0.04 Hz; post stimulus: 0.57 ± 0.07 Hz; $n = 12/15$; K–S Test; $P = 0.0068$; Fig. 4a2), and a significant reduction in their amplitude (26.0 ± 7.4 % of control; pre stimulus: 46.0 ± 2.1 pA; post stimulus: 33.0 ± 2.3 pA; $n = 12/15$; $P = 0.0015$; Fig. 4a3). To determine whether CB1R stimulation was mediating this change, we performed the same stimulation in the presence of the CB1R antagonist AM251. In a previous study, we have found that within the LDT, bath application of AM251 alone results in an increase in the frequency of sIPSCs (Soni et al. 2014), which is an effect shown in other brain regions as well, such as the hippocampus (Hentges et al. 2005; Losonczy et al. 2004; Neu et al. 2007) and amygdala (Roberto et al. 2010; Zhu and Lovinger 2005) and this action occurred in the present study as well. However, pre-incubation of the slice in AM251 (2 min) abolished the ability of depolarization of the cell to decrease the AM251-heightened frequency (only 3.5 ± 2.9 % change of control; pre-stimulus: 1.1 ± 0.27 Hz; poststimulus: 1.2 ± 0.26 Hz; $n = 4/4$; $P = 0.4294$; Fig. 4b2) and amplitude of sIPSCs in patch-clamped LDT neurons (13.0 ± 6.8 % reduced from control; pre stimulus: 48.0 ± 4.9 pA; post stimulus: 42.0 ± 5.7 pA; $n = 4/4$; $P = 0.1123$; Fig. 4b3). These data indicate that eCBs can be produced within the LDT, which corroborates our earlier findings of endogenous production in the brain slice limiting ongoing IPSC activity, and further, our present data indicate that depolarization of LDT neurons can result in a positive feedback signal reducing inhibitory drive directed to these cells.

DSI is sensitive to the Ca^{2+} chelator BAPTA

In some cell types, DSI has been found to rely on rises in $[Ca^{2+}]_i$ (Ohno-Shosaku et al. 2002; Varma et al. 2001),

whereas in other regions, DSI can occur as a Ca^{2+}-independent process (Kim et al. 2002). We wished to determine whether the DSI induced by direct depolarization of LDT cells was dependent on Ca^{2+}. Accordingly, we conducted a series of recordings using patch pipettes filled with the Ca^{2+} chelator BAPTA, which is highly selective for Ca^{2+} over Mg^{2+}, and a more rapid Ca^{2+} buffer than EGTA (Tsien 1980). After establishment of a seal onto the cell surface and rupture of the membrane, the pipette contents were allowed to equilibrate with the intracellular contents, allowing BAPTA diffusion throughout the neuronal processes. Following a period of equilibration, the depolarizing step protocol was applied to the LDT neuron. We found that BAPTA completely blocked the reduction in frequency of IPSCs induced by the depolarizing step ($2.4 \pm 7.6 \%$ reduced from control; pre stimulus: 0.56 ± 0.05 Hz; post stimulus: 0.54 ± 0.04 Hz; $n = 7/9$; $P = 0.5590$; Fig. 4c2) in the majority of cells studied and the reduction in sIPSC amplitude induced by direct depolarization of these neurons was also abolished (no change $102.9 \pm 5.7 \%$ of control; pre stimulus: 48.0 ± 2.9 pA; post stimulus: 49.0 ± 3.3 pA; $n = 7/9$; $P = 0.6780$; Fig. 4c3). As we did not have an internal control for presence of DSI in the cells before BAPTA exposure, we conducted a non-parametric test to determine whether there was a significant difference in the numbers of cells exhibiting DSI in control conditions and those failing to exhibit this phenomenon in presence of BAPTA. Our data indicated that there was a significant difference in the rate of occurrence of DSI in control cells from that occurring during the BAPTA recording conditions (responsive cells in absence of BAPTA: 12/15 (80 %); responsive cells in presence of BAPTA: 2/9 (22 %); $P = 0.0104$, Fisher Exact test, two tailed). Our findings indicate that Ca^{2+} chelation prevented a significant change in frequency and amplitude of sIPSCc after direct depolarization, which suggests that rises in $[Ca^{2+}]_i$ are involved in induction of DSI in LDT neurons.

As a major source of activity-dependent intracellular Ca^{2+} increase in LDT cells is influx via L-type Ca^{2+} channels, we investigated the role of the L-type Ca^{2+} channel in the Ca^{2+}-dependent DSI. In the presence of bath-applied nifedipine, direct depolarization failed to induce a significant change in the frequency of sIPSCs ($P = 0.4312$, $n = 3/3$, Fig. 4c4), however, a small, significant change in the amplitude was noted ($P = 0.0392$, $n = 3/3$, Fig. 4c5). Following wash out of the nifedipine from two of the three brain slices previously exposed, two more cells were patched and direct depolarization induced a change in frequency which was similar to that seen in control conditions (36.6 % of control, $n = 2$, data not shown). These data suggest that L-type Ca^{2+} channels play a role in eCB production stimulated by depolarization.

The metabotropic glutamate receptor (mGluR) agonist, DHPG, induces DSI in the LDT

Endogenous activation of eCBs has been shown to occur upon activation of mGluRs and this activation can induce DSI (Chevaleyre and Castillo 2003; Glitsch et al. 1996; Maejima et al. 2001; Morishita et al. 1998; Puente et al. 2011; Varma et al. 2001). Recently, we presented work showing that the Group I, type I, metabotropic glutamate receptors (mGlu1R) are present on LDT neurons, and when activated, can stimulate rises in $[Ca^{2+}]_i$ (Kohlmeier et al. 2006, 2013). Further, we demonstrated the presence of a local glutamate circuit within the LDT which exhibited ongoing activity in the brain slice (Kohlmeier et al. 2012). Taken together, these data suggest that the endogenous release of glutamate in the LDT from local neurons or terminals of projection neurons (Honda and Semba 1995) could induce DSI via actions on mGluRs on cells in this nucleus. In our earlier study, recording conditions were not optimized to detect whether the application of mGluR1 agonists affected the frequency or amplitude of sIPSCs that we have shown are mediated in LDT cells by GABAergic mechanisms (Ishibashi et al. 2009). Therefore, we conducted a new series of experiments with high chloride-containing pipettes and inclusion in the ACSF of blockers of ionotropic glutamate receptors, and monitored the actions of the mGlu1R agonist, DHPG, on synaptic activity to determine whether stimulation of the mGlu1R elicited DSI in LDT cells (Fig. 5a1). In patch-clamped LDT neurons, bath application of DHPG (50 μM; 2–3 min) inhibited the frequency of sIPSCs ($32.0 \pm 6.5 \%$ reduced from control; con: 0.75 ± 0.11 Hz; DHPG: 0.48 ± 0.05; $n = 5/5$; $P = 0.0148$; Fig. 5a2) as well as reduced their amplitude ($17 \pm 5.1 \%$ reduced from control; con: 47.0 ± 5.6 pA; DHPG: 39.0 ± 4.3 pA; $n = 5/5$; K–S test; $P = 0.0365$; Fig. 5a3). As activation of mGlu1Rs can induce release of Ca^{2+} from intracellular stores in LDT cells, and this Ca^{2+} may be involved in mGlu1R mediated DSI, we examined whether DHPG-stimulated DSI was a Ca^{2+}-dependent process. Inclusion of BAPTA in the patch pipette eliminated the DHPG-induced change in frequency ($n = 7/7$; $P = 0.1409$; Fig. 5b2) and amplitude ($n = 7/7$; $P = 0.9973$; Fig. 5b3) of sIPSCs suggesting the requirement of rises in intracellular Ca^{2+} in induction of mGluR-elicited DSI.

Effects included the involvement of the CB1R since the DHPG action on the frequency and amplitude of sIPSCs was sensitive to preincubation (2–3 min) of the slice in AM251. In the presence of AM251, DHPG failed to induce an inhibition in frequency of sIPSCs ($3.2 \pm 3.0 \%$ reduced from control; con: 0.93 ± 0.08 Hz; DHPG: 0.89 ± 0.06 Hz; $n = 4/4$; K–S test; $P = 0.0347$; Fig. 5b4) and the reduction in amplitude was not elicited ($5.3 \pm 4.8 \%$ reduced from control; con: 29 ± 3.2 pA;

A 1 AP5 + DNQX   Post-Stimulus

50 pA
60 s

2

3

B 1 AP5 + DNQX + AM251   Post-Stimulus

50 pA
60 s

2   3

In AM251   In AM251

C 1 AP5 + DNQX + BAPTA   Post-Stimulus

50 pA
60 s

2   3   4   5

In BAPTA   In BAPTA   In Nifedipine   In Nifedipine
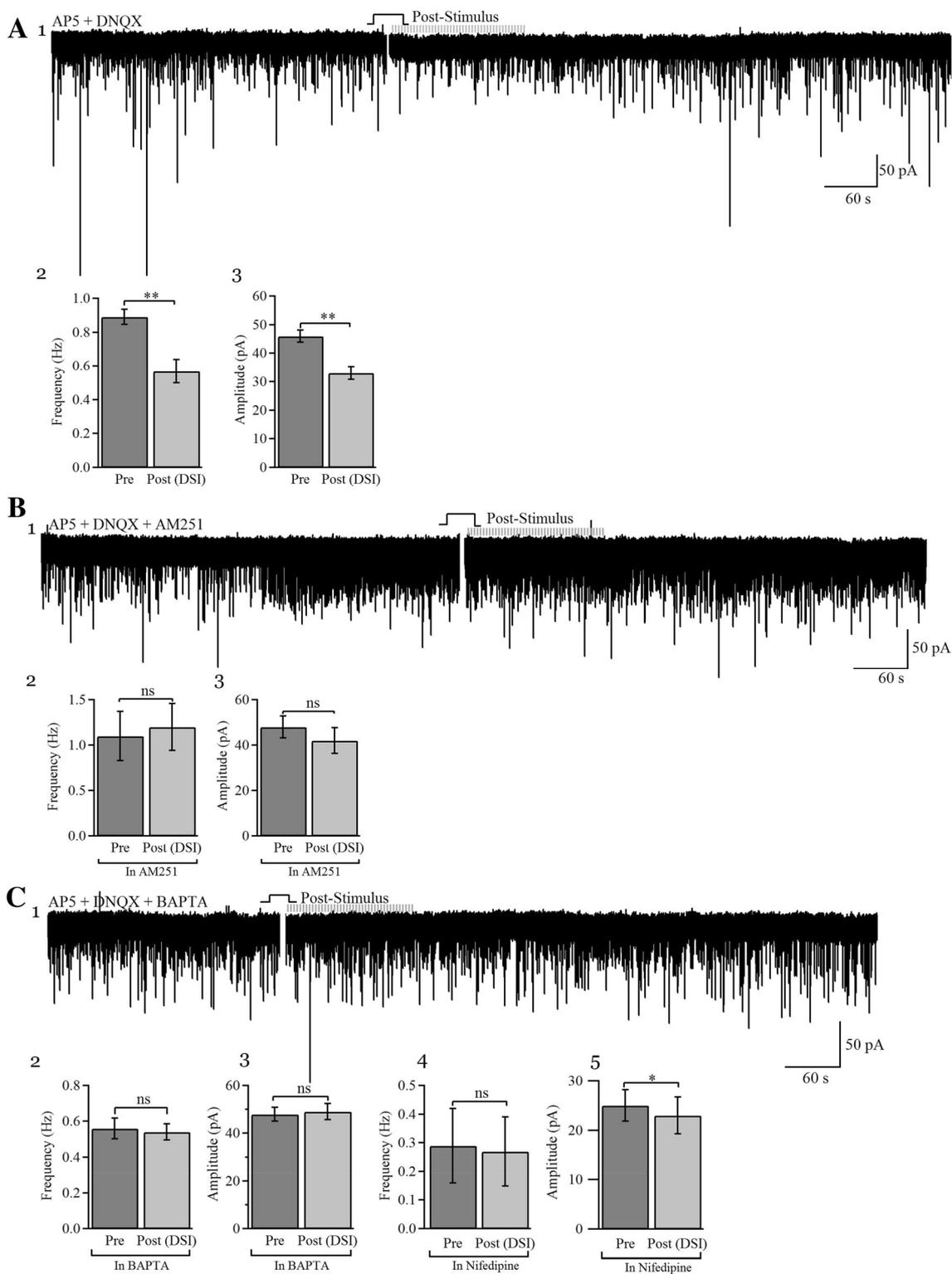
DHPG: 27 ± 2.1 pA; $n = 4/4$; $P = 0.0233$; Fig. 5b5). In a group of cells, we examined the effect of DHPG on the frequency and amplitude of IPSCs in the presence of TTX to block action potential generation in the slice (Fig. 5c1). In the presence of TTX, DHPG reduced the frequency of mIPSCs (43 ± 3.8 % of control; con: 0.55 ± 0.09 Hz; DHPG: 0.32 ± 0.06 Hz; $n = 4/4$; $P = 0.0090$; Fig. 5c2), but did not significantly affect the amplitude of these inhibitory events (5.1 ± 3.7 % of

◄**Fig. 4** Depolarization-induced suppression of inhibition (DSI) of spontaneous inhibitory currents (IPSCs) within the LDT nucleus. **a1** An individual voltage recording of a patch-clamped LDT neuron displaying DSI induced by application of a depolarizing voltage step (0 mV for 10 s) from the resting holding potential of −60 mV. DSI following the voltage step (poststimulus, 120 s) is clearly seen in that the frequency and amplitude of IPSCs (downward deflections) are reduced. Blockers of ionotropic glutamate receptors are present in these recordings. Histograms from the population of neurons studied in which it can be seen that there was a significant decrease in both the frequency (**a2**) and amplitude (**a3**) of IPSCs following the stimulation, when compared with that pre-stimulus. **b1** A voltage recording from another neuron showing the failure to induce DSI in the presence of the CB1R antagonist AM251. Presence of AM251 inhibited any significant stimulus-induced change in the frequency (**b2**) or amplitude (**b2**) of IPSCs in the population of LDT neurons studied. **c** A representative voltage recording of a LDT neuron recorded with BAPTA (20 mM) in the patch solution illustrating that DSI was not induced in this cell by the depolarization step when the Ca^{2+} chelator was present. The majority of the LDT cells recorded with BAPTA-containing pipettes failed to show a stimulation-induced significant inhibition of the frequency (**c2**) or amplitude of sIPSCs (**c3**), indicating that DSI induced by a depolarizing step is dependent on $[Ca^{2+}]_i$. (**c4**) When nifedipine was added to the bath, the frequency (**c4**) of IPSCs failed to be significantly changed by a depolarizing step, however, the amplitude was still reduced (**c5**). These data suggest a role of Ca^{2+} flux via L-type Ca^{2+} channels in depolarization-induced DSI. *Error bars* indicating the SEM. *indicates $P < 0.05$, **indicates $P < 0.001$ and 'ns' designates no significant difference

control; con: 50.0 ± 3.9 pA; DHPG: 47.0 ± 2.4 pA; $n = 4/4$; $P = 0.2579$; Fig. 5c3). In the presence of AM251 (Fig. 5d1), DHPG had no significant effect on mIPSC frequency (5.3 ± 8.3 % of control; con: 0.46 ± 0.09 Hz; DHPG: 0.42 ± 0.08 Hz; $n = 8/8$; $P = 0.3656$; Fig. 5d2) or amplitude (6.3 ± 7.8 % of control; con: 42 ± 4.1 pA; DHPG: 44 ± 4.5 pA; $n = 8$; $P = 0.6186$; Fig. 5d3). When taken together, these data suggest a presynaptic localization for the relevant CB1Rs. In a few cells, establishment of the recovery of the control levels of sIPSC frequency and amplitude indicated that actions were not due to cell run down ($n = 3$). Taken together, these data indicate that the activation of mGlu1Rs is capable of inducing DSI in a Ca^{2+}-dependent process and suggest that endogenous activation of these receptors by demonstrated glutamatergic input directed to LDT cells could result in disinhibition thereby, altering the excitability of these cells.

Immunohistochemistry was used to identify recorded cells from the LDT nucleus

We were only able to recover a total of 15 cells from imaging studies using patch-clamp recordings upon which immunohistochemistry could be performed. In studies monitoring the effects of WIN-2 on $\Delta F/F$ %, two of the 15 recorded and recovered cells were found to be bNOS positive (one of them shown in Fig. 6a1, 2), indicating that the majority of cells recovered were non cholinergic (one of them shown in Fig. 6b1, 2). Six of the 15 cells recovered were included in the studies examining the antagonizing actions of AM251. Of these 6, only one cell out of those recovered was found to be both bNOS and Alexa-594 positive; whereas, 5 recovered recorded cells in this study were determined to be non cholinergic. Our data suggest that rises in $[Ca^{2+}]_i$ induced by CB1R agonism occur both in cholinergic and non-cholinergic neurons and, as our sample size was too small to make firm conclusions, future studies will need to be conducted to determine whether responses occur preferentially within any particular LDT phenotype. Further, a very recent study raises the possibility that rises in Ca^{2+} can be triggered in glial cells in the brain stem by CB1R activation (Koszeghy et al. 2014) and while the Alexa-594 cells were identified as neurons in this study, future studies could be conducted to examine whether CB1Rs on glial cells in the LDT play a role in cellular processes in this nucleus.

Discussion

Ca^{2+} imaging and electrophysiology recordings presented in this study provide strong evidence that activation of CB1Rs results in rises in Ca^{2+} in LDT cells. WIN-2-induced increases in fluorescence indicative of rises in Ca^{2+} were apparent in both AM-loaded LDT cells, in which the intracellular milieu had not been disturbed, and in single LDT neurons using patch-clamp recordings. While some rises in Ca^{2+} in postsynaptic neurons were dependent upon synaptic transmission and, therefore, blocked by low Ca^{2+} or presence of TTX, a significant proportion of the rises in Ca^{2+} was sensitive to depletion of SERCA-pumps, indicating that the source of these Ca^{2+} transients was likely release from intracellular stores. A very similar phenomenon has been observed in hippocampal neurons in which activation of the CB1R leads to increases in cytosolic Ca^{2+} and these rises in $[Ca^{2+}]_i$ were diminished by the Ca^{2+}-ATPase inhibitor, CPA (Isokawa and Alger 2005; 2006). Rises in $[Ca^{2+}]_i$ induced by the CB1R agonist were sensitive to a CB1R antagonist, AM251, further suggesting that actions of WIN-2 were specific to the activation of CB1Rs, rather than non-receptor mediated effects. These data are in agreement with findings in NG108-15 and N18TG2 cells showing that direct CB1R stimulation using THC and 2-arachidonoyl glycerol induced a modest increase in $[Ca^{2+}]_i$ (Kondo et al. 1998; Sugiura et al. 1997), which was sensitive to the CB1R antagonist, SR141716A (Rinaldi-Carmona et al. 1995).

While the stimulation of presynaptic CB1Rs also leads to rises in Ca^{2+} in postsynaptic LDT cells, we chose to
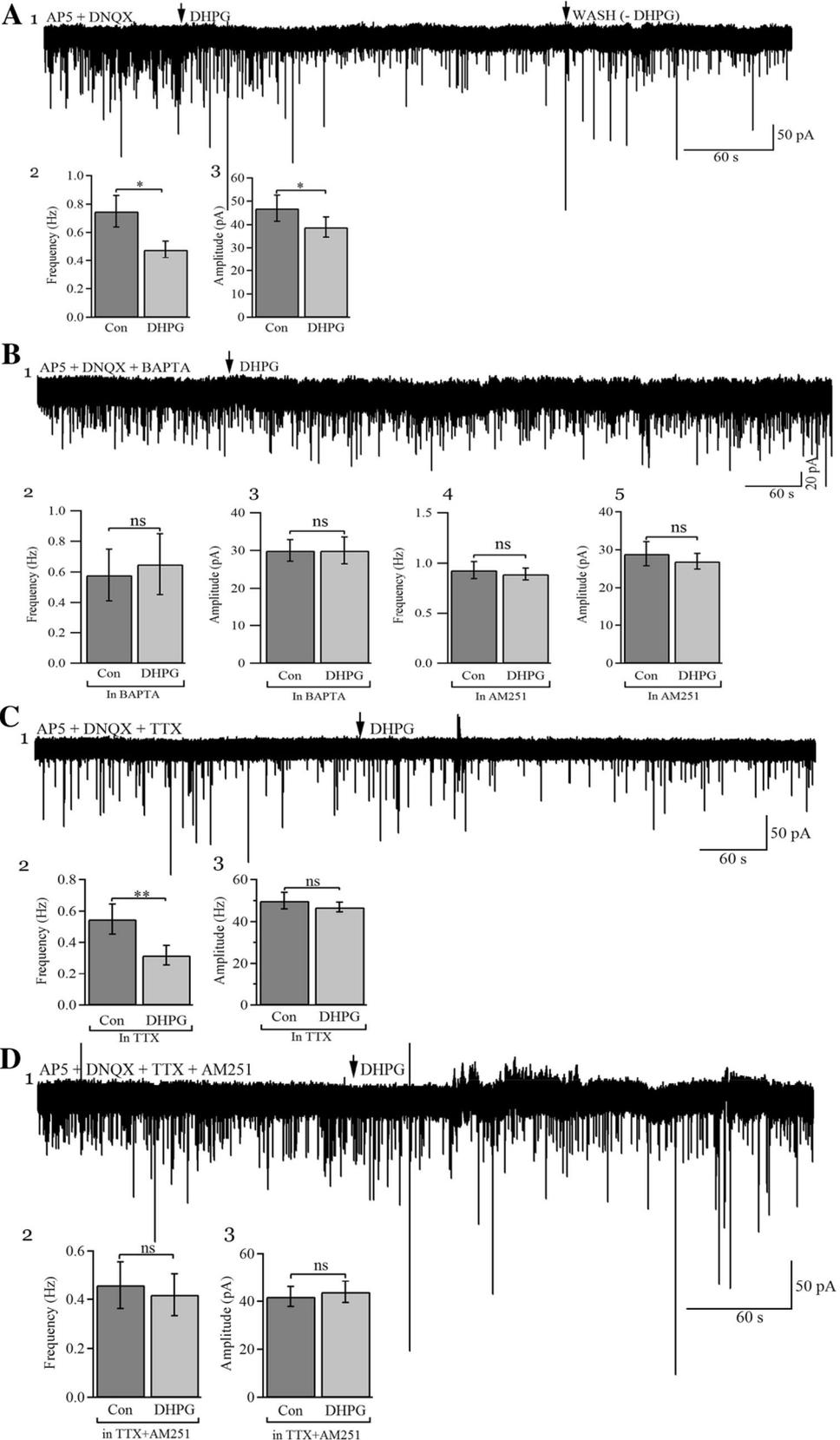
◄**Fig. 5** mGluR activation induced suppression of inhibition of IPSCs within neurons of the LDT. DHPG, a potent Group I, type 1, mGluR agonist was used in this study. **a1** A representative voltage recording from an individual LDT neuron showing that bath application of DHPG reduced the frequency and amplitude of sIPSCs. Upon washout of DHPG, some initial recovery of the cell from this action is apparent. DHPG significantly reduced the frequency (**a2**) and amplitude (**a3**) of sIPSCs in the population of neurons examined within the LDT. **b1** Inclusion of BAPTA in the patch pipette eliminated mGluR-induced changes in the frequency and amplitude of sIPSCs, as can be seen in this representative recording from a LDT neuron, and in the histograms of the summary data taken from a population of recorded cells (**b2, 3**). Pre-incubation of the slice with AM251 significantly inhibited the DHPG-induced change in frequency (**b4**) and amplitude (**b5**) of IPSCs in a population of LDT cells, indicating involvement of the CB1R. When taken together, these data indicate that mGluR stimulation leads to Ca^{2+}-dependent DSI involving the CB1R. **c1** Recording from a representative LDT neuron in TTX indicating that DHPG is effective in reducing the frequency, but not the amplitude of mIPSCs. In a group of LDT cells, DHPG induced a significant change in frequency (**c2**) but not in the amplitude (**c3**) of mIPSCs. **d1** Pre-incubation of LDT cells with the bath-applied CB1R antagonist, AM251, inhibited the DHPG-induced change in frequency of mIPSCs, which is apparent from this voltage recording from a single LDT neuron in which TTX is present. **d2** Histogram showing the effect of DHPG on mIPSC frequency when applied in the presence of AM251 in a population of LDT neurons. DHPG failed to induce any significant change in frequency or in amplitude (**d3**) of mIPSCs in LDT neurons when the CB1R antagonist was present. Taken together, these data suggest a CB1R-mediated, presynaptic effect induced by activation of mGluR1 s in the LDT. *Error bars* indicating the SEM. *indicates $P < 0.05$ and **indicates $P < 0.001$ and 'ns' designates no significant difference

focus our studies on the Ca^{2+} rises insensitive to synaptic blockade. However, Ca^{2+} rises sourcing from activation of CB1Rs located presynaptically and away from the terminals is likely importantly involved in functioning of the postsynaptic cell (Glass and Felder 1997; Howlett et al. 2002, 2004; Matsuda et al. 1990). Ca^{2+} plays a fundamental role in activation of gene regulation and in synaptic plasticity and the eCB system has been recognized to mediate many forms of synaptic plasticity in the postsynaptic cell following presynaptic stimulation (Glass and Felder 1997; Heifets and Castillo 2009; Howlett et al. 2004). Therefore, although it was not explored in the present study, it remains of interest what are the underlying mechanisms of the rises in Ca^{2+} sensitive to synaptic blockade and what is the role played in the postsynaptic cell of these rises.

There are several caveats of our studies which examined changes in Ca^{2+}. Our imaging studies were conducted in young animals, however, studies have shown that the CB1R is present in the rodent brain during development and in the early postnatal period and that production of endogenous agonists of this receptor, such as anandamide, occurs during this time (Berrendero et al. 1999; Fernandez-Ruiz et al. 1999). Further, CB1R mRNA levels in the

brainstem were highest during this developmental period. Of course, other involved effectors, such as ion channels may not be at adult levels. However, a previous study of another G-protein-mediated action (mGluR), which involved the inwardly rectifying potassium channel in LDT cells did show that this action extended to neurons in brain slices from animals of a similar age to those in the present study (Kohlmeier et al. 2013), suggesting that at least some ion channels present in the adult, are present at an early age in the LDT. Further, in a preliminary study, we performed some recordings in cells from older animals (16–25 days of age), which showed that DSI induced by direct depolarization ($n = 3$ cells) and by DHPG ($n = 1$) occurs in LDT neurons from this range of ages (K–S test, $P < 0.05$). Accordingly, although it remains to be tested, we believe CB1R phenomenon noted in the present work extends beyond the range of ages examined.

Another caveat of our study was that we choose to use an indirect measure of Ca^{2+}, rather than directly record Ca^{2+} currents. Our choice of Ca^{2+} imaging was deliberate, as previous experience indicated that recordings of LDT cells would not survive for the long periods of time required for this study if they were held under conditions necessary for isolation of Ca^{2+} currents. Ca^{2+} imaging has been conducted in other neuronal types and changes in fluorescence of Ca^{2+} binding dyes have been shown to exhibit a strong correlation with depolarising voltage shifts expected to trigger rises in $Ca^{2+,}$ and data from these studies have been presented as functional evidence allowing conclusions regarding cellular processes leading to Ca^{2+} rises (Isope and Murphy 2005; Murphy et al. 1995; Regehr et al. 1989; Sargoy et al. 2014). Further, we have shown in LDT neurons that voltage protocols resulting in depolarization of the membrane result in rises in fluorescence, which are sensitive to selective Ca^{2+} channel antagonists (Kohlmeier and Leonard 2006). Although direct measures of Ca^{2+} should be conducted to confirm our findings obtained with Ca^{2+} sensing dyes, we do believe our data support the conclusion that CB1R activation results in calcium rises in LDT neurons. Another caveat of our study is that we were unable to definitively establish in which neuronal type effects extended in the majority of cases. Immunohistochemistry from single cell recordings revealed that these effects occurred in cholinergic and non-cholinergic LDT neurons. The LDT is a mixed population of glutamatergic, cholinergic and GABAergic neurons (Wang and Morales 2009) with some size distinction in that glutamate and cholinergic cells tend to be larger than the GABAergic cells (Boucetta and Jones 2009). As there is currently no reliable electrophysiological way to unambiguously distinguish the different LDT neuronal phenotypes, using optical guidance, we targeted cells appearing to be larger than 15 μm. A sampling of total cell
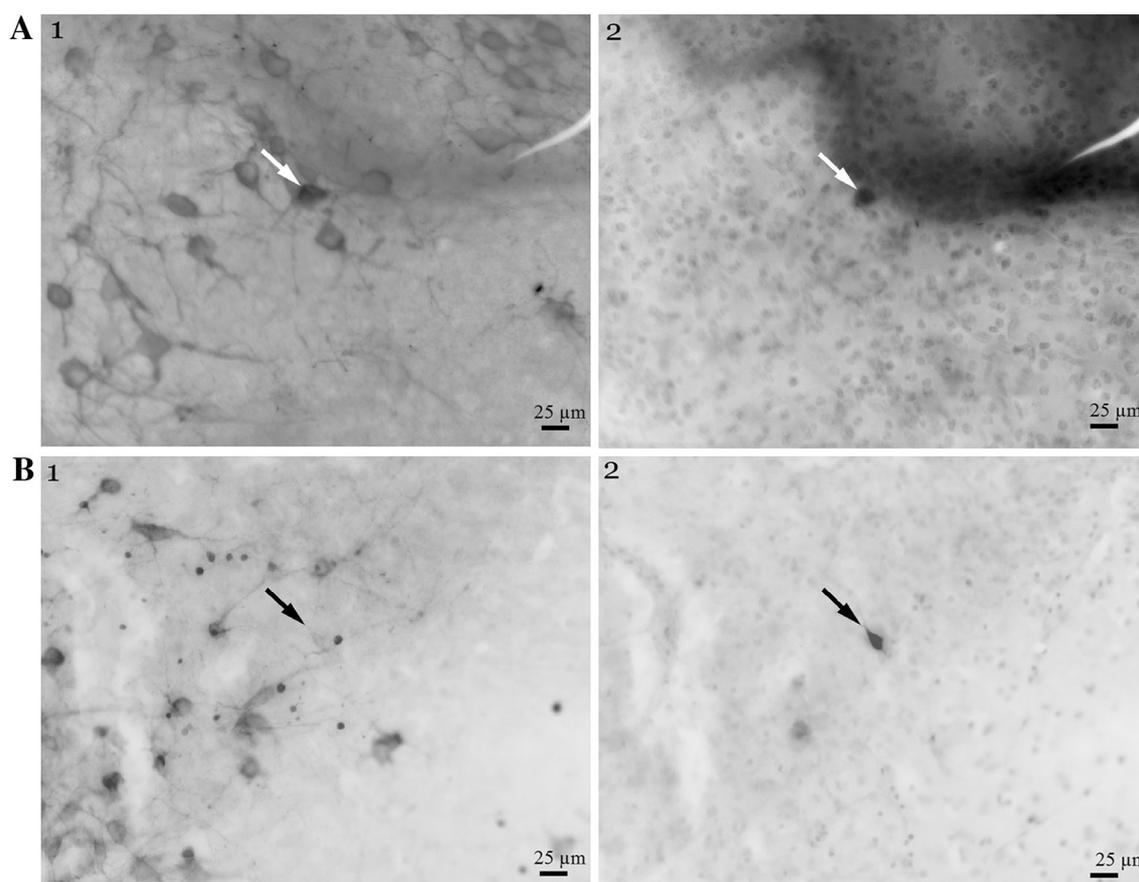
Fig. 6 Immunohistochemical identification of patch-clamped cells: **a1** following immunohistochemical processing of the brain slice, bNOS positive cells are visible under appropriate fluorescence (488 nM). (**a2**) Cells from which recordings sourced could be identified by presence of Alexa-594. Coincidence of bNOS and Alexa-594 in the same cell indicated that the recorded cell was cholinergic as shown by this representative LDT neuron which responded to WIN-2 with a rise in $[Ca^{2+}]_i$ (*white arrows* in **a1** and **a2**). **b** Failure to co-localize these two fluorescent indicators indicated that a recorded neuron was non cholinergic as shown in this example of an Alexa-594 containing cell (**b2**, *black arrow*) which responded to WIN-2 with a rise in $[Ca^{2+}]_i$ but was negative for presence of bNOS (**b1**)

capacitance in a subpopulation of cells in the present study provided further support for the conclusion that recordings derived from large cells (41.16 + 1.8 pF; $n = 19$ cells). With the caveat that long recording times could have dialysed bNOS, leading to false negative cell identifications, our immunohistochemistry further supports the interpretation that it is highly likely that our population of large, non cholinergic recorded neurons included a significant population of glutamate cells. When taken together, it is tempting to speculate that within the LDT, in addition to CB1R functional presence on cholinergic and GABA-releasing LDT terminals as indicated by findings in our previous study (Soni et al. 2014), these receptors are also present on glutamatergic neurons in this nucleus. Findings from a previous study did indicate that CB1R-mediated DSE was present in two LDT cells suggesting presence of CB1Rs on glutamatergic LDT neurons, however, DSE was not elicited in the majority of recorded cells. Agonist

concentration was speculated to have not been high enough to activate DSE in the majority of cells (Soni et al. 2014). When taken together, it remains a possibility that CB1Rs are present on glutamate LDT cells, and therefore, that eCB-mediated rises in $[Ca^{2+}]_i$ in these cells could play a role in processes controlled by this LDT phenotype. However, identification of the exact neurotransmitter content of the population of non-cholinergic LDT neurons exhibiting CB1R-mediated rises in $[Ca^{2+}]_i$ remains for future investigations.

A recent report presented evidence for CB1R on glial cells in a cholinergic nucleus adjacent to the LDT, the pedunculopontine tegmentum (PPT). Using a different Ca^{2+} imaging dye, CB1R-mediated rises in calcium were detected in glial cells of the PPT (Koszeghy et al. 2014) which raises the possibility that imaged cells in the present study included non neurons. However, in the present study using a dye that has previously been shown

to load neurons in the LDT (Kohlmeier et al. 2004) and by targeting large cells in this nucleus unlikely to be glia which are less than 10 μm, and by confirming WIN-2-mediated rises in $\Delta F/F$ occurred in cells which exhibited action potentials, we do believe CB1R-mediated Ca^{2+} rises occur in neurons of the LDT. Although we do not rule out occurrence of CB1R-mediated rises in glial cells of this nucleus, rises in Ca^{2+} with the kinetics of slow Ca^{2+} waves which were typical of CB1R-mediated Ca^{2+} in PPT glial cells, and glia in other neuronal regions (Koszeghy et al. 2014; Takahashi et al. 2007), were not detected in any of the cells imaged in the present study, lending further support to our conclusion that neurons of the LDT do exhibit CB1R-mediated rises in Ca^{2+}. A proportion of rises in Ca^{2+} in the LDT were insensitive to TTX and low Ca^{2+} conditions, but were sensitive to SERCA-pump depletion. Interestingly, WIN-2-mediated rises in Ca^{2+} in PPT glial cells were also SERCA-pump sensitive and Ca^{2+} sourcing from this store was associated with release of glutamate, which, in a novel finding, was found to act at postsynaptic mGluRs (Koszeghy et al. 2014). As we have shown that mGluR stimulation leads to rises in Ca^{2+} in postsynaptic LDT cells (Kohlmeier et al. 2013), there is a possibility that Ca^{2+} rises seen in the present study were mediated by a similar phenomenon. However, arguing against a CB1R-mediated increase in glutamate as a mechanism underlying the present data is our earlier study which failed to find any evidence of an enhancement of glutamate release when CB1Rs in the LDT were stimulated (Soni et al. 2014). Regardless, while postsynaptic CB1Rs likely mediate TTX and low Ca^{2+} insensitive, and SERCA-pump sensitive rises in Ca^{2+} seen in the present study, it remains a possibility that CB1Rs on LDT glial cells contribute to these rises.

DSI within LDT

In our study, we also found that direct depolarization of LDT neurons lead to a reduction in the frequency and amplitude of sIPSCs directed to LDT neurons, which is a phenomenon noted in other cells types to be mediated by the eCB system (DSI). This DSI was mediated by CB1 receptors as the CB1R antagonist, AM251, blocked this action. This is the first time that DSI has been shown within the LDT. As a rise in $[Ca^{2+}]_i$ is vital for eCB synthesis, it is no surprise that numerous studies have shown that rises in $[Ca^{2+}]_i$ are a prerequisite for eCB-mediated DSI (Isokawa and Alger 2005; Lenz and Alger 1999; Morishita and Alger 1997; Ohno-Shosaku et al. 2005; Pitler and Alger 1992; Wilson and Nicoll 2001). However, some studies indicate that while eCB synthesis requires rises in $[Ca^{2+}]_i$, release of eCBs is independent of this $[Ca^{2+}]_i$ rise (Kim et al. 2002). Our findings show that DSI was sensitive to

chelation of $[Ca^{2+}]_i$ suggesting that DSI induced by depolarization is dependent on $[Ca^{2+}]_i$ levels. Blockade of the voltage-gated L-type Ca^{2+} channel eliminated the reduction in frequency of IPSCs induced by direct depolarization, suggesting a role of this Ca^{2+} channel in this phenomenon as has been seen in other neuronal types. Depolarization-activated DSI was shown in hippocampal neurons to be mediated by the N-, and in certain situations, the L-type Ca^{2+} channel (Lenz et al. 1998) and DSI can be enhanced by L-type Ca^{2+} channel modulators (Pitler and Alger 1992). While our findings implicate a role of the L-type Ca^{2+} channel in DSI, our data do not rule out involvement of other voltage-operated Ca^{2+} channels in DSI, nor that other stimuli that induce DSI in the LDT may do so in a Ca^{2+}-independent fashion. Alternatively, Ca^{2+} required may source independent of flux across the membrane.

mGluRs activation as a source of DSI within LDT

Numerous studies suggest that pharmacological and electrophysiological activation of metabotropic glutamate or muscarinic receptors can induce the formation of eCBs that mediate retrograde synaptic signals (Brenowitz and Regehr 2003; Kim et al. 2002; Ohno-Shosaku et al. 2003) which suppresses the release of neurotransmission. In the present study, we showed that activation of mGluRs leads to DSI, which could be mediated by rises in $[Ca^{2+}]_i$ as we have previously shown that stimulation of this receptor leads to intracellular release of Ca^{2+} in LDT neurons (Kohlmeier et al. 2004). Previously, it had been shown that activation of mGluRs leads to eCB-mediated retrograde signaling in the hippocampus (Chevaleyre and Castillo 2003; Morishita et al. 1998; Varma et al. 2001), amygdala, NAc, and in the cerebellum (Glitsch et al. 1996; Puente et al. 2011; Robbe et al. 2002). However, our data are the first to show mGluR-mediated DSI in the LDT, and that this DSI requires Ca^{2+} in the postsynaptic cell. Our data therefore extend the literature regarding brain regions where stimulation of the mGluR triggers eCB-mediated signaling. Further, our data showing an elimination of the DHPG-induced increase in amplitude of mIPSCs, without a change in the increase in frequency in presence of TTX, suggests that CB1Rs mediating this action are located presynaptic to the recorded cell and within the terminal. The ability of BAPTA to eliminate pharmacological DSI suggests that eCBs are produced in the postsynaptic cell. Based on previous data (Kohlmeier et al. 2013), the source of Ca^{2+}-mediating mGluR DSI was likely to source from mGluR-stimulated release from intracellular Ca^{2+} stores. In the present work, we were focused on the elucidation of DSI as our previous findings showed WIN-2-mediated decreases in IPSCs, therefore, we included blockers of ionotropic

glutamate receptors in our recordings designed to examine DSI. While in our previous study, we did not note an action of WIN-2 on enhancing or suppressing EPSC activity in the majority of cells examined, suggesting that CB1R stimulation does not lead to alterations in synaptic glutamate release, we cannot rule out that eCB stimulation in the LDT does not lead to this phenomenon; therefore, it would be of interest to directly examine whether eCB-dependent DSE exists within the neurons of the LDT.

Inhibition of L-type Ca^{2+} channels

Another functional outcome of the activation of the CB1R within the LDT was the reduction in Ca^{2+} currents mediated by the L-type Ca^{2+} channel heavily present in cells of this nucleus. eCB-mediated inhibition of L-type Ca^{2+} currents has also been reported in vertebrate retinal bipolar neurons (Straiker et al. 1999; Straiker and Sullivan 2003). While the role played by eCB-mediated inhibition of the L-type Ca^{2+} channel in LDT cells was not examined, the CB1R-mediated reductions in activity of this Ca^{2+} conductance would be expected to modulate synaptic transmission (Hell et al. 1993; Lipscombe et al. 2004; Ludwig et al. 1997) as decreases in L-type Ca^{2+} channel activity have been shown to lead to inhibition of synaptic vesicle release in other cells. In addition, L-type Ca^{2+} channels have been shown to be involved in mechanisms underlying synaptic plasticity (Huang and Malenka 1993; Kullmann et al. 1992; Norris et al. 1998; Weisskopf et al. 1999). eCB signaling within the LDT via actions on the L-type Ca^{2+} channel present could regulate synaptic transmission in this nucleus and shape output to terminal regions via inhibition of conductance through this channel. Interestingly, depolarization-induced DSI was shown to involve Ca^{2+} influx via L-type Ca^{2+} channels. Although there could be differences in actions when using pharmacological vs physiological stimulation of CB1Rs, it is worth considering that activity-dependent production of eCBs by the postsynaptic cell could serve as a feedback inhibitory mechanism, limiting Ca^{2+} influx via voltage-operated L-type Ca^{2+} channels. This effect would depend on the location of effectors at which eCBs act relative to where they are released.

Functional significance

The LDT is a heterogeneous nucleus, comprised of GABAergic, glutamatergic and cholinergic neurons (Wang and Morales 2009) with a subpopulation of neurons synthesizing both GABA and ACh (Jia et al. 2003). As we targeted cells larger than 15 μm in this nucleus, it is highly likely our population of recorded cells sourced not only from the cholinergic cells of this nucleus but also the glutamatergic cells (Boucetta et al. 2014; Boucetta and

Jones 2009), although this point was not established. The cholinergic neurons have been well characterized as playing a pivotal role in control of behavioral states exhibiting cortical arousal and phenomenology of REM sleep and in accordance with this role, show their highest firing activity during alert wakefulness and REM sleep which is likely involved in the gamma-frequency rich, activated EEG pattern common to these two behavioral states (el Mansari et al. 1989; Jones and Webster 1988; Kayama et al. 1992; Steriade et al. 1990; Thakkar et al. 1998; Webster and Jones 1988; Williams et al. 1994). The glutamate neurons of the LDT also exhibit state-dependent firing and while their role in state control is less well understood, it is likely they do participate in modulation of behavioral state (Boucetta et al. 2014). Cholinergic along with glutamate neurons of the LDT are also importantly involved in motivated states via demonstrated projections to the VTA (Lammel et al. 2012; Omelchenko and Sesack 2005) and the NAc (Dautan et al. 2014). Input from the LDT drives firing patterns in the VTA leading to behaviourally significant rises in dopamine (DA) in target regions of the NAc (Lodge and Grace 2006). High DA efflux in the NAc is associated with the assignment of reward to stimuli, including drugs of abuse, and is associated with behavioral signs of addiction (Drevets et al. 2001; Pontieri et al. 1995) Accordingly, activity of the LDT is likely to participate in assigning stimuli saliency which is supported by findings that optogenetic stimulation specifically of the LDT-VTA pathway induces addiction-like behaviors in absence of a drug cue (Lammel et al. 2012). Given the roles played by the LDT, elucidation of the mechanisms controlling cellular excitability of LDT cells is necessary if we are to completely understand how behavioral states exhibiting an aroused EEG are controlled and how external stimuli induce motivation. Emerging from our current studies are findings indicating that the activation of CB1Rs in the LDT leads to inhibition of GABAergic transmission and that activation of glutamatergic neurons and terminals leading to release of glutamate within the LDT could result in inhibition of GABAergic release within this nucleus (Fig. 7). Further, activation of CB1Rs alters Ca^{2+} dynamics in LDT cells, which among other mechanisms, could influence cellular plasticity and synaptic transmission. Exogenous use of marijuana and its psychoactive constituents (i.e., THC), which are agonists at the CB1R, can lead to the development of addictive behaviors, and, their use has also been linked to disturbances in sleep patterns (Feinberg et al. 1975, 1976; Pivik et al. 1972) and levels of alertness during wakefulness (Nicholson et al. 2004) suggesting that cellular effects seen in the present study could play a role in these behavioral actions.

The actions of stimulation of the CB1R on inhibiting L-type Ca^{2+} channels in the LDT are of functional interest
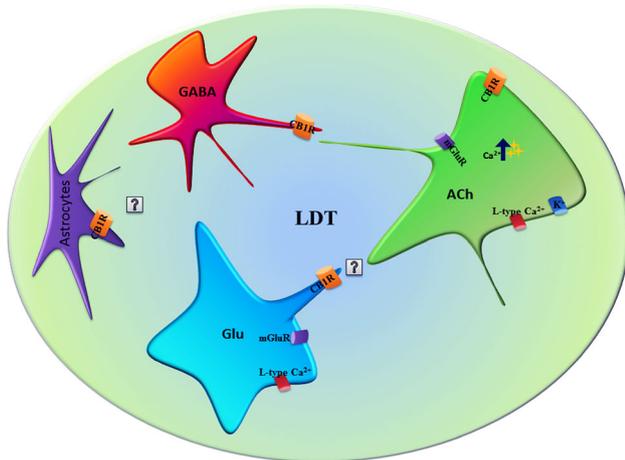
Fig. 7 Proposed schematic of the location of CB1Rs in the LDT and effectors at which exogenous or endogenous ligands of these receptors act. Our previous studies provided evidence for presence of CB1Rs on terminals located on GABAergic cells (*red cell*) presynaptic to cholinergic neurons (*green cell*) as well as postsynaptic CB1Rs linked to activation of potassium channels on cholinergic neurons (Soni et al. 2014). The present study provides evidence for CB1Rs located on non cholinergic neurons (bNOS negative), which based on their size quite likely include glutamate-containing cells (*blue cell*), although this point remains to be established. Our data also showed effects of CB1Rs which were reliant on action potential generation suggesting a presynaptic presence of CB1Rs located farther away than the terminal, however, the location of these receptors was not examined. Also not addressed in this study, the possibility exists that CB1Rs could be located on glial cells of the LDT (*violet cell*), as has been reported in the PPT, an adjacent cholinergic nucleus (Koszeghy et al. 2014). Effectors influenced by eCB actions were studied. L-type Ca^{2+} channels have previously been shown to be present on LDT cells (Kohlmeier and Leonard 2006), and in this study, were shown to be modulated by CB1 agonists, and also involved in production of DSI induced by direct depolarization, which was a Ca^{2+}-dependent process. Previous work established presence of ongoing, locally sourced glutamate tone in LDT brainslices (Kohlmeier et al. 2012) and presence of mGlu1Rs on LDT cells which were linked to release of Ca^{2+} from intracellular stores (Kohlmeier et al. 2013). In this study, pharmacological DSI could be induced by mGlu1R agonists, in non-identified cells, which was a process dependent on intracellular Ca^{2+}

when considering that these channels are currently drug targets for the treatment of many diseases. The $Ca_v1.2$ and the $Ca_v1.3$ represent the brain's predominant L-type Ca^{2+} channel (Catterall et al. 2005) and both have been shown to be present in neurons of the LDT (Ishibashi et al. 2010). Both subtypes have been shown to be involved in depression and behavioral responses to drugs of abuse (Giordano et al. 2010; Wankerl et al. 2010), and reductions in the activity of L-type Ca^{2+} channels have been suggested as a theoretical therapeutic approach in the management of neurodegenerative diseases such as Parkinson's Disease by reducing oxidative stress (Guzman et al. 2010; Rivero-Rios et al. 2014), which is interesting in light of the degeneration present within the cholinergic mesopontine tegmentum

early in this progressive disease (Zweig et al. 1989). While we did not directly address at which L-type Ca^{2+} channel subtype the effects of CB1R receptor activation extended, previous work indicates that the $Ca_v1.3$ subunit contributes the majority of Ca^{2+} induced by a voltage step to -30 mV, as was used in the present study (Ishibashi et al. 2010). Our data provide the intriguing possibility that altering eCB transmission could be an approach if targeting the L-type Ca^{2+} channels, particularly those containing the $Ca_v1.3$ subunit, in the LDT. Regardless, activation of the CB1R via endogenous or exogenous mechanisms would be expected to result in inhibition of this channel within the LDT, which would likely have a large impact on synaptic functioning of these cells, influencing their control of arousal and appetitive behaviors. Taken together, our data elucidating the cellular actions of functional CB1Rs in the LDT with an emphasis on processes leading to alterations in $[Ca^{2+}]_i$ provide further knowledge regarding how marijuana could exert its behavioral actions on alert wakefulness, stages of sleep, and motivated states and suggest that endogenous eCBs could play a role in the neural control of wakefulness and aroused, goal-driven states.

References

Alger BE, Kim J (2011) Supply and demand for endocannabinoids. Trends Neurosci 34:304–315

Allen Mouse Brain Atlas [Internet] (2012) Allen Institute for Brain Science. http://mouse.brain-map.org/. Accessed 7 July 2014

Berrendero F, Garcia-Gil L, Hernandez ML, Romero J, Cebeira M, de Miguel R, Ramos JA, Fernandez-Ruiz JJ (1998) Localization of mRNA expression and activation of signal transduction mechanisms for cannabinoid receptor in rat brain during fetal development. Development 125:3179–3188

Berrendero F, Sepe N, Ramos JA, Di Marzo V, Fernandez-Ruiz JJ (1999) Analysis of cannabinoid receptor binding and mRNA expression and endogenous cannabinoid contents in the developing rat brain during late gestation and early postnatal period. Synapse 33:181–191

Boucetta S, Jones BE (2009) Activity profiles of cholinergic and intermingled GABAergic and putative glutamatergic neurons in the pontomesencephalic tegmentum of urethane-anesthetized rats. J Neurosci 29:4664–4674

Boucetta S, Cisse Y, Mainville L, Morales M, Jones BE (2014) Discharge profiles across the sleep-waking cycle of identified

cholinergic, GABAergic, and glutamatergic neurons in the pontomesencephalic tegmentum of the rat. J Neurosci 34:4708–4727

Brenowitz SD, Regehr WG (2003) Calcium dependence of retrograde inhibition by endocannabinoids at synapses onto Purkinje cells. J Neurosci 23:6373–6384

Brown SP, Safo PK, Regehr WG (2004) Endocannabinoids inhibit transmission at granule cell to Purkinje cell synapses by modulating three types of presynaptic calcium channels. J Neurosci 24:5623–5631

Burkey TH, Quock RM, Consroe P, Ehlert FJ, Hosohata Y, Roeske WR, Yamamura HI (1997) Relative efficacies of cannabinoid CB1 receptor agonists in the mouse brain. Eur J Pharmacol 336:295–298

Catterall WA, Perez-Reyes E, Snutch TP, Striessnig J (2005) International Union of Pharmacology. XLVIII. Nomenclature and structure-function relationships of voltage-gated calcium channels. Pharmacol Rev 57:411–425

Caulfield MP, Brown DA (1992) Cannabinoid receptor agonists inhibit Ca current in NG108-15 neuroblastoma cells via a pertussis toxin-sensitive mechanism. Br J Pharmacol 106:231–232

Chevaleyre V, Castillo PE (2003) Heterosynaptic LTD of hippocampal GABAergic synapses: a novel role of endocannabinoids in regulating excitability. Neuron 38:461–472

Christensen MH, Ishibashi M, Nielsen ML, Leonard CS, Kohlmeier KA (2014) Age-related changes in nicotine response of cholinergic and non-cholinergic laterodorsal tegmental neurons: Implications for the heightened adolescent susceptibility to nicotine addiction. Neuropharmacology 85:263–283

Compton DR, Gold LH, Ward SJ, Balster RL, Martin BR (1992) Aminoalkylindole analogs: cannabimimetic activity of a class of compounds structurally distinct from delta 9-tetrahydrocannabinol. J Pharmacol Exp Ther 263:1118–1126

Dautan D, Huerta-Ocampo I, Witten IB, Deisseroth K, Bolam JP, Gerdjikov T, Mena-Segovia J (2014) A major external source of cholinergic innervation of the striatum and nucleus accumbens originates in the brainstem. J Neurosci 34:4509–4518

Devane WA, Hanus L, Breuer A, Pertwee RG, Stevenson LA, Griffin G, Gibson D, Mandelbaum A, Etinger A, Mechoulam R (1992) Isolation and structure of a brain constituent that binds to the cannabinoid receptor. Science 258:1946–1949

Diana MA, Levenes C, Mackie K, Marty A (2002) Short-term retrograde inhibition of GABAergic synaptic currents in rat Purkinje cells is mediated by endogenous cannabinoids. J Neurosci 22:200–208

Drevets WC, Gautier C, Price JC, Kupfer DJ, Kinahan PE, Grace AA, Price JL, Mathis CA (2001) Amphetamine-induced dopamine release in human ventral striatum correlates with euphoria. Biol Psychiatry 49:81–96

Edwards DA, Kim J, Alger BE (2006) Multiple mechanisms of endocannabinoid response initiation in hippocampus. J Neurophysiol 95:67–75

el Mansari M, Sakai K, Jouvet M (1989) Unitary characteristics of presumptive cholinergic tegmental neurons during the sleep-waking cycle in freely moving cats. Exp Brain Res 76:519–529

Endoh T (2006) Pharmacological characterization of inhibitory effects of postsynaptic opioid and cannabinoid receptors on calcium currents in neonatal rat nucleus tractus solitarius. Br J Pharmacol 147:391–401

Feinberg I, Jones R, Walker JM, Cavness C, March J (1975) Effects of high dosage delta-9-tetrahydrocannabinol on sleep patterns in man. Clin Pharmacol Ther 17:458–466

Feinberg I, Jones R, Walker J, Cavness C, Floyd T (1976) Effects of marijuana extract and tetrahydrocannabinol on electroencephalographic sleep patterns. Clin Pharmacol Ther 19:782–794

Fergusson DM, Horwood LJ (2000) Does cannabis use encourage other forms of illicit drug use? Addiction 95:505–520

Fernandez-Ruiz JJ, Berrendero F, Hernandez ML, Romero J, Ramos JA (1999) Role of endocannabinoids in brain development. Life Sci 65:725–736

Forster GL, Blaha CD (2000) Laterodorsal tegmental stimulation elicits dopamine efflux in the rat nucleus accumbens by activation of acetylcholine and glutamate receptors in the ventral tegmental area. Eur J Neurosci 12:3596–3604

Freund TF, Katona I, Piomelli D (2003) Role of endogenous cannabinoids in synaptic signaling. Physiol Rev 83:1017–1066

Gaoni Y, Mechoulam R (1964) Isolation, structure, and partial synthesis of an active constituent of hashish. J Am Chem Soc 86:1646

Gatley SJ, Gifford AN, Volkow ND, Lan R, Makriyannis A (1996) 123I-labeled AM251: a radioiodinated ligand which binds in vivo to mouse brain cannabinoid CB1 receptors. Eur J Pharmacol 307:331–338

Gatley SJ, Lan R, Pyatt B, Gifford AN, Volkow ND, Makriyannis A (1997) Binding of the non-classical cannabinoid CP 55,940, and the diarylpyrazole AM251 to rodent brain cannabinoid receptors. Life Sci 61:PL191–PL197

Giordano TP, Tropea TF, Satpute SS, Sinnegger-Brauns MJ, Striessnig J, Kosofsky BE, Rajadhyaksha AM (2010) Molecular switch from L-type Ca v 1.3 to Ca v 1.2 Ca^{2+} channel signaling underlies long-term psychostimulant-induced behavioral and molecular plasticity. J Neurosci 30:17051–17062

Glass M, Felder CC (1997) Concurrent stimulation of cannabinoid CB1 and dopamine D2 receptors augments cAMP accumulation in striatal neurons: evidence for a Gs linkage to the CB1 receptor. J Neurosci 17:5327–5333

Glitsch M, Llano I, Marty A (1996) Glutamate as a candidate retrograde messenger at interneurone-Purkinje cell synapses of rat cerebellum. J Physiol 497(Pt 2):531–537

Guzman JN, Sanchez-Padilla J, Wokosin D, Kondapalli J, Ilijic E, Schumacker PT, Surmeier DJ (2010) Oxidant stress evoked by pacemaking in dopaminergic neurons is attenuated by DJ-1. Nature 468:696–700

Heifets BD, Castillo PE (2009) Endocannabinoid signaling and long-term synaptic plasticity. Annu Rev Physiol 71:283–306

Hell JW, Westenbroek RE, Warner C, Ahlijanian MK, Prystay W, Gilbert MM, Snutch TP, Catterall WA (1993) Identification and differential subcellular localization of the neuronal class C and class D L-type calcium channel alpha 1 subunits. J Cell Biol 123:949–962

Hentges ST, Low MJ, Williams JT (2005) Differential regulation of synaptic inputs by constitutively released endocannabinoids and exogenous cannabinoids. J Neurosci 25:9746–9751

Honda T, Semba K (1995) An ultrastructural study of cholinergic and non-cholinergic neurons in the laterodorsal and pedunculopontine tegmental nuclei in the rat. Neuroscience 68:837–853

Hope BT, Michael GJ, Knigge KM, Vincent SR (1991) Neuronal NADPH diaphorase is a nitric oxide synthase. Proc Natl Acad Sci USA 88:2811–2814

Howlett AC (2005) Cannabinoid receptor signaling. Handb Exp Pharmacol 168:53–79

Howlett AC, Barth F, Bonner TI, Cabral G, Casellas P, Devane WA, Felder CC, Herkenham M, Mackie K, Martin BR, Mechoulam R, Pertwee RG (2002) International Union of Pharmacology. XXVII. Classification of cannabinoid receptors. Pharmacol Rev 54:161–202

Howlett AC, Breivogel CS, Childers SR, Deadwyler SA, Hampson RE, Porrino LJ (2004) Cannabinoid physiology and pharmacology: 30 years of progress. Neuropharmacology 47(Suppl 1):345–358

Huang YY, Malenka RC (1993) Examination of TEA-induced synaptic enhancement in area CA1 of the hippocampus: the role of voltage-dependent Ca^{2+} channels in the induction of LTP. J Neurosci 13:568–576

Ishibashi M, Leonard CS, Kohlmeier KA (2009) Nicotinic activation of laterodorsal tegmental neurons: implications for addiction to nicotine. Neuropsychopharmacology 34:2529–2547

Ishibashi M, Gumenchuk I, Leonard CS (2010) L-type calcium channels containing CaV 1.3 contribute to voltage-dependent calcuim influx in mouse laterodorsal tegmental neurons. Soc Neurosci (Abstract) 35

Isokawa M, Alger BE (2005) Retrograde endocannabinoid regulation of GABAergic inhibition in the rat dentate gyrus granule cell. J Physiol 567:1001–1010

Isokawa M, Alger BE (2006) Ryanodine receptor regulates endogenous cannabinoid mobilization in the hippocampus. J Neurophysiol 95:3001–3011

Isope P, Murphy TH (2005) Low threshold calcium currents in rat cerebellar Purkinje cell dendritic spines are mediated by T-type calcium channels. J Physiol 562:257–269

Iversen L (2003) Cannabis and the brain. Brain 126:1252–1270

Jia HG, Yamuy J, Sampogna S, Morales FR, Chase MH (2003) Colocalization of gamma-aminobutyric acid and acetylcholine in neurons in the laterodorsal and pedunculopontine tegmental nuclei in the cat: a light and electron microscopic study. Brain Res 992:205–219

Jones BE, Webster HH (1988) Neurotoxic lesions of the dorsolateral pontomesencephalic tegmentum-cholinergic cell area in the cat. I. Effects upon the cholinergic innervation of the brain. Brain Res 451:13–32

Jones BE, Yang TZ (1985) The efferent projections from the reticular formation and the locus coeruleus studied by anterograde and retrograde axonal transport in the rat. J Comp Neurol 242:56–92

Kayama Y, Ohta M, Jodo E (1992) Firing of 'possibly' cholinergic neurons in the rat laterodorsal tegmental nucleus during sleep and wakefulness. Brain Res 569:210–220

Kim J, Isokawa M, Ledent C, Alger BE (2002) Activation of muscarinic acetylcholine receptors enhances the release of endogenous cannabinoids in the hippocampus. J Neurosci 22:10182–10191

Kohlmeier KA, Leonard CS (2006) Transmitter modulation of spike-evoked calcium transients in arousal related neurons: muscarinic inhibition of SNX-482-sensitive calcium influx. Eur J Neurosci 23:1151–1162

Kohlmeier KA, Inoue T, Leonard CS (2004) Hypocretin/orexin peptide signaling in the ascending arousal system: elevation of intracellular calcium in the mouse dorsal raphe and laterodorsal tegmentum. J Neurophysiol 92:221–235

Kohlmeier KA, Soja PJ, Kristensen MP (2006) Disparate cholinergic currents in rat principal trigeminal sensory nucleus neurons mediated by M1 and M2 receptors: a possible mechanism for selective gating of afferent sensory neurotransmission. Eur J Neurosci 23:3245–3258

Kohlmeier KA, Watanabe S, Tyler CJ, Burlet S, Leonard CS (2008) Dual orexin actions on dorsal raphe and laterodorsal tegmentum neurons: noisy cation current activation and selective enhancement of Ca^{2+} transients mediated by L-type calcium channels. J Neurophysiol 100:2265–2281

Kohlmeier KA, Ishibashi M, Wess J, Bickford ME, Leonard CS (2012) Knockouts reveal overlapping functions of M(2) and M(4) muscarinic receptors and evidence for a local glutamatergic circuit within the laterodorsal tegmental nucleus. J Neurophysiol 108:2751–2766

Kohlmeier KA, Christensen MH, Kristensen MP, Kristiansen U (2013) Pharmacological evidence of functional inhibitory metabotrophic glutamate receptors on mouse arousal-related cholinergic laterodorsal tegmental neurons. Neuropharmacology 66:99–113

Kondo S, Kondo H, Nakane S, Kodaka T, Tokumura A, Waku K, Sugiura T (1998) 2-Arachidonoylglycerol, an endogenous cannabinoid receptor agonist: identification as one of the major species of monoacylglycerols in various rat tissues, and evidence for its generation through Ca^{2+} -dependent and -independent mechanisms. FEBS Lett 429:152–156

Koszeghy A, Kovacs A, Biro T, Szucs P, Vincze J, Hegyi Z, Antal M, Pal B (2014) Endocannabinoid signaling modulates neurons of the pedunculopontine nucleus (PPN) via astrocytes. Brain Struct Funct. doi:10.1007/s00429-014-0842-5

Kreitzer AC, Regehr WG (2001) Retrograde inhibition of presynaptic calcium influx by endogenous cannabinoids at excitatory synapses onto Purkinje cells. Neuron 29:717–727

Kullmann DM, Perkel DJ, Manabe T, Nicoll RA (1992) Ca^{2+} entry via postsynaptic voltage-sensitive Ca^{2+} channels can transiently potentiate excitatory synaptic transmission in the hippocampus. Neuron 9:1175–1183

Lammel S, Lim BK, Ran C, Huang KW, Betley MJ, Tye KM, Deisseroth K, Malenka RC (2012) Input-specific control of reward and aversion in the ventral tegmental area. Nature 491:212–217

Lauckner JE, Hille B, Mackie K (2005) The cannabinoid agonist WIN55,212-2 increases intracellular calcium via CB1 receptor coupling to Gq/11 G proteins. Proc Natl Acad Sci USA 102:19144–19149

Lauckner JE, Jensen JB, Chen HY, Lu HC, Hille B, Mackie K (2008) GPR55 is a cannabinoid receptor that increases intracellular calcium and inhibits M current. Proc Natl Acad Sci USA 105:2699–2704

Lenz RA, Alger BE (1999) Calcium dependence of depolarization-induced suppression of inhibition in rat hippocampal CA1 pyramidal neurons. J Physiol 521(Pt 1):147–157

Lenz RA, Wagner JJ, Alger BE (1998) N- and L-type calcium channel involvement in depolarization-induced suppression of inhibition in rat hippocampal CA1 cells. J Physiol 512(Pt 1):61–73

Lipscombe D, Helton TD, Xu W (2004) L-type calcium channels: the low down. J Neurophysiol 92:2633–2641

Lodge DJ, Grace AA (2006) The laterodorsal tegmentum is essential for burst firing of ventral tegmental area dopamine neurons. Proc Natl Acad Sci USA 103:5167–5172

Losonczy A, Biro AA, Nusser Z (2004) Persistently active cannabinoid receptors mute a subpopulation of hippocampal interneurons. Proc Natl Acad Sci USA 101:1362–1367

Ludwig A, Flockerzi V, Hofmann F (1997) Regional expression and cellular localization of the alpha1 and beta subunit of high voltage-activated calcium channels in rat brain. J Neurosci 17:1339–1349

Mackie K, Hille B (1992) Cannabinoids inhibit N-type calcium channels in neuroblastoma-glioma cells. Proc Natl Acad Sci USA 89:3825–3829

Mackie K, Lai Y, Westenbroek R, Mitchell R (1995) Cannabinoids activate an inwardly rectifying potassium conductance and inhibit Q-type calcium currents in AtT20 cells transfected with rat brain cannabinoid receptor. J Neurosci 15:6552–6561

Maejima T, Hashimoto K, Yoshida T, Aiba A, Kano M (2001) Presynaptic inhibition caused by retrograde signal from metabotropic glutamate to cannabinoid receptors. Neuron 31:463–475

Mailleux P, Vanderhaeghen JJ (1992) Distribution of neuronal cannabinoid receptor in the adult rat brain: a comparative receptor binding radioautography and in situ hybridization histochemistry. Neuroscience 48:655–668

Matsuda LA, Lolait SJ, Brownstein MJ, Young AC, Bonner TI (1990) Structure of a cannabinoid receptor and functional expression of the cloned cDNA. Nature 346:561–564

Matsuda LA, Bonner TI, Lolait SJ (1993) Localization of cannabinoid receptor mRNA in rat brain. J Comp Neurol 327:535–550

Mechoulam R, Ben-Shabat S, Hanus L, Ligumsky M, Kaminski NE, Schatz AR, Gopher A, Almog S, Martin BR, Compton DR et al (1995) Identification of an endogenous 2-monoglyceride, present in canine gut, that binds to cannabinoid receptors. Biochem Pharmacol 50:83–90

Melis M, Pistis M, Perra S, Muntoni AL, Pillolla G, Gessa GL (2004) Endocannabinoids mediate presynaptic inhibition of glutamatergic transmission in rat ventral tegmental area dopamine neurons through activation of CB1 receptors. J Neurosci 24:53–62

Min R, Di Marzo V, Mansvelder HD (2010) DAG lipase involvement in depolarization-induced suppression of inhibition: does endocannabinoid biosynthesis always meet the demand? Neuroscientist 16:608–613

Morishita W, Alger BE (1997) Sr^{2+} supports depolarization-induced suppression of inhibition and provides new evidence for a presynaptic expression mechanism in rat hippocampal slices. J Physiol 505(Pt 2):307–317

Morishita W, Kirov SA, Alger BE (1998) Evidence for metabotropic glutamate receptor activation in the induction of depolarization-induced suppression of inhibition in hippocampal CA1. J Neurosci 18:4870–4882

Murphy TH, Baraban JM, Wier WG (1995) Mapping miniature synaptic currents to single synapses using calcium imaging reveals heterogeneity in postsynaptic output. Neuron 15:159–168

Naraghi M (1997) T-jump study of calcium binding kinetics of calcium chelators. Cell Calcium 22:255–268

Neher E (1992) Correction for liquid junction potentials in patch clamp experiments. Methods Enzymol 207:123–131

Nelson CL, Wetter JB, Milovanovic M, Wolf ME (2007) The laterodorsal tegmentum contributes to behavioral sensitization to amphetamine. Neuroscience 146:41–49

Neu A, Foldy C, Soltesz I (2007) Postsynaptic origin of CB1-dependent tonic inhibition of GABA release at cholecystokinin-positive basket cell to pyramidal cell synapses in the CA1 region of the rat hippocampus. J Physiol 578:233–247

Nicholson AN, Turner C, Stone BM, Robson PJ (2004) Effect of Delta-9-tetrahydrocannabinol and cannabidiol on nocturnal sleep and early-morning behavior in young adults. J Clin Psychopharmacol 24:305–313

Norris CM, Halpain S, Foster TC (1998) Reversal of age-related alterations in synaptic plasticity by blockade of L-type Ca^{2+} channels. J Neurosci 18:3171–3179

Ohno-Shosaku T, Shosaku J, Tsubokawa H, Kano M (2002) Cooperative endocannabinoid production by neuronal depolarization and group I metabotropic glutamate receptor activation. Eur J Neurosci 15:953–961

Ohno-Shosaku T, Matsui M, Fukudome Y, Shosaku J, Tsubokawa H, Taketo MM, Manabe T, Kano M (2003) Postsynaptic M1 and M3 receptors are responsible for the muscarinic enhancement of retrograde endocannabinoid signalling in the hippocampus. Eur J Neurosci 18:109–116

Ohno-Shosaku T, Hashimotodani Y, Maejima T, Kano M (2005) Calcium signaling and synaptic modulation: regulation of endocannabinoid-mediated synaptic modulation by calcium. Cell Calcium 38:369–374

Omelchenko N, Sesack SR (2005) Laterodorsal tegmental projections to identified cell populations in the rat ventral tegmental area. J Comp Neurol 483:217–235

Omelchenko N, Sesack SR (2006) Cholinergic axons in the rat ventral tegmental area synapse preferentially onto mesoaccumbens dopamine neurons. J Comp Neurol 494:863–875

Oz M (2006a) Receptor-independent actions of cannabinoids on cell membranes: focus on endocannabinoids. Pharmacol Ther 111:114–144

Oz M (2006b) Receptor-independent effects of endocannabinoids on ion channels. Curr Pharm Des 12:227–239

Perra S, Pillolla G, Melis M, Muntoni AL, Gessa GL, Pistis M (2005) Involvement of the endogenous cannabinoid system in the effects of alcohol in the mesolimbic reward circuit: electrophysiological evidence in vivo. Psychopharmacology 183:368–377

Pitler TA, Alger BE (1992) Postsynaptic spike firing reduces synaptic GABAAA responses in hippocampal pyramidal cells. J Neurosci 12:4122–4132

Pivik RT, Zarcone V, Dement WC, Hollister LE (1972) Delta-9-tetrahydrocannabinol and synhexl: effects on human sleep patterns. Clin Pharmacol Ther 13:426–435

Pontieri FE, Tanda G, Di Chiara G (1995) Intravenous cocaine, morphine, and amphetamine preferentially increase extracellular dopamine in the "shell" as compared with the "core" of the rat nucleus accumbens. Proc Natl Acad Sci USA 92:12304–12308

Puente N, Cui Y, Lassalle O, Lafourcade M, Georges F, Venance L, Grandes P, Manzoni OJ (2011) Polymodal activation of the endocannabinoid system in the extended amygdala. Nat Neurosci 14:1542–1547

Regehr WG, Connor JA, Tank DW (1989) Optical imaging of calcium accumulation in hippocampal pyramidal cells during synaptic activation. Nature 341:533–536

Rinaldi-Carmona M, Barth F, Heaulme M, Alonso R, Shire D, Congy C, Soubrie P, Breliere JC, Le Fur G (1995) Biochemical and pharmacological characterisation of SR141716A, the first potent and selective brain cannabinoid receptor antagonist. Life Sci 56:1941–1947

Rivero-Rios P, Gomez-Suaga P, Fdez E, Hilfiker S (2014) Upstream deregulation of calcium signaling in Parkinson's disease. Front Mol Neurosci 7:53

Robbe D, Alonso G, Duchamp F, Bockaert J, Manzoni OJ (2001) Localization and mechanisms of action of cannabinoid receptors at the glutamatergic synapses of the mouse nucleus accumbens. J Neurosci 21:109–116

Robbe D, Kopf M, Remaury A, Bockaert J, Manzoni OJ (2002) Endogenous cannabinoids mediate long-term synaptic depression in the nucleus accumbens. Proc Natl Acad Sci USA 99:8384–8388

Robbe D, Alonso G, Manzoni OJ (2003) Exogenous and endogenous cannabinoids control synaptic transmission in mice nucleus accumbens. Ann N Y Acad Sci 1003:212–225

Robbe D, Montgomery SM, Thome A, Rueda-Orozco PE, McNaughton BL, Buzsaki G (2006) Cannabinoids reveal importance of spike timing coordination in hippocampal function. Nat Neurosci 9:1526–1533

Roberto M, Cruz M, Bajo M, Siggins GR, Parsons LH, Schweitzer P (2010) The endocannabinoid system tonically regulates inhibitory transmission and depresses the effect of ethanol in central amygdala. Neuropsychopharmacology 35:1962–1972

Sargoy A, Sun X, Barnes S, Brecha NC (2014) Differential calcium signaling mediated by voltage-gated calcium channels in rat retinal ganglion cells and their unmyelinated axons. PLoS One 9:e84507

Satoh K, Fibiger HC (1986) Cholinergic neurons of the laterodorsal tegmental nucleus: efferent and afferent connections. J Comp Neurol 253:277–302

Serrano A, Parsons LH (2011) Endocannabinoid influence in drug reinforcement, dependence and addiction-related behaviors. Pharmacol Ther 132:215–241

Soni N, Satpathy S, Kohlmeier KA (2014) Neurophysiological Evidence for the Presence of Cannabinoid CB1 receptors in the Laterodorsal Tegmental Nucleus: a New Aspect of Neuronal Control of Marijuana Addiction and States of Arousal. Eur J Neurosci 40:3635–3652

Steriade M, Datta S, Pare D, Oakson G, Curro Dossi RC (1990) Neuronal activities in brain-stem cholinergic nuclei related to tonic activation processes in thalamocortical systems. J Neurosci 10:2541–2559

Straiker A, Sullivan JM (2003) Cannabinoid receptor activation differentially modulates ion channels in photoreceptors of the tiger salamander. J Neurophysiol 89:2647–2654

Straiker A, Stella N, Piomelli D, Mackie K, Karten HJ, Maguire G (1999) Cannabinoid CB1 receptors and ligands in vertebrate retina: localization and function of an endogenous signaling system. Proc Natl Acad Sci USA 96:14565–14570

Sugiura T, Kondo S, Sukagawa A, Nakane S, Shinoda A, Itoh K, Yamashita A, Waku K (1995) 2-Arachidonoylglycerol: a possible endogenous cannabinoid receptor ligand in brain. Biochem Biophys Res Commun 215:89–97

Sugiura T, Kodaka T, Kondo S, Nakane S, Kondo H, Waku K, Ishima Y, Watanabe K, Yamamoto I (1997) Is the cannabinoid CB1 receptor a 2-arachidonoylglycerol receptor? Structural requirements for triggering a Ca^{2+} transient in NG108-15 cells. J Biochem 122:890–895

Sugiura T, Kodaka T, Nakane S, Miyashita T, Kondo S, Suhara Y, Takayama H, Waku K, Seki C, Baba N, Ishima Y (1999) Evidence that the cannabinoid CB1 receptor is a 2-arachidonoylglycerol receptor. Structure-activity relationship of 2-arachidonoylglycerol, ether-linked analogues, and related compounds. J Biol Chem 274:2794–2801

Takahashi A, Camacho P, Lechleiter JD, Herman B (1999) Measurement of intracellular calcium. Physiol Rev 79:1089–1125

Takahashi N, Sasaki T, Usami A, Matsuki N, Ikegaya Y (2007) Watching neuronal circuit dynamics through functional multi-neuron calcium imaging (fMCI). Neurosci Res 58:219–225

Thakkar MM, Strecker RE, McCarley RW (1998) Behavioral state control through differential serotonergic inhibition in the mesopontine cholinergic nuclei: a simultaneous unit recording and microdialysis study. J Neurosci 18:5490–5497

Tsien RY (1980) New calcium indicators and buffers with high selectivity against magnesium and protons: design, synthesis, and properties of prototype structures. Biochemistry 19:2396–2404

Tsou K, Brown S, Sanudo-Pena MC, Mackie K, Walker JM (1998) Immunohistochemical distribution of cannabinoid CB1 receptors in the rat central nervous system. Neuroscience 83:393–411

Varma N, Carlson GC, Ledent C, Alger BE (2001) Metabotropic glutamate receptors drive the endocannabinoid system in hippocampus. J Neurosci 21:RC188

Vincent SR, Satoh K, Armstrong DM, Fibiger HC (1983) NADPH-diaphorase: a selective histochemical marker for the cholinergic neurons of the pontine reticular formation. Neurosci Lett 43:31–36

Wang HL, Morales M (2009) Pedunculopontine and laterodorsal tegmental nuclei contain distinct populations of cholinergic, glutamatergic and GABAergic neurons in the rat. Eur J Neurosci 29:340–358

Wankerl K, Weise D, Gentner R, Rumpf JJ, Classen J (2010) L-type voltage-gated Ca^{2+} channels: a single molecular switch for long-term potentiation/long-term depression-like plasticity and activity-dependent metaplasticity in humans. J Neurosci 30:6197–6204

Webster HH, Jones BE (1988) Neurotoxic lesions of the dorsolateral pontomesencephalic tegmentum-cholinergic cell area in the cat. II. Effects upon sleep-waking states. Brain Res 458:285–302

Weisskopf MG, Bauer EP, LeDoux JE (1999) L-type voltage-gated calcium channels mediate NMDA-independent associative long-term potentiation at thalamic input synapses to the amygdala. J Neurosci 19:10512–10519

Williams JA, Comisarow J, Day J, Fibiger HC, Reiner PB (1994) State-dependent release of acetylcholine in rat thalamus measured by in vivo microdialysis. J Neurosci 14:5236–5242

Wilson RI, Nicoll RA (2001) Endogenous cannabinoids mediate retrograde signalling at hippocampal synapses. Nature 410:588–592

Wilson RI, Kunos G, Nicoll RA (2001) Presynaptic specificity of endocannabinoid signaling in the hippocampus. Neuron 31:453–462

Zhu PJ, Lovinger DM (2005) Retrograde endocannabinoid signaling in a postsynaptic neuron/synaptic bouton preparation from basolateral amygdala. J Neurosci 25:6199–6207

Zweig RM, Jankel WR, Hedreen JC, Mayeux R, Price DL (1989) The pedunculopontine nucleus in Parkinson's disease. Ann Neurol 26:41–46